



A Conceptual Model for Projecting Coccolithophorid Growth, Calcification and Photosynthetic Carbon Fixation Rates in Response to Global Ocean Change

Natasha A. Gafar*, Bradley D. Eyre and Kai G. Schulz

Centre for Coastal Biogeochemistry, School of Environment Science and Engineering, Southern Cross University, Lismore, NSW, Australia

OPEN ACCESS

Edited by:

Agostino Merico,
Leibniz Centre for Tropical Marine
Research (LG), Germany

Reviewed by:

Peng Jin,
King Abdullah University of Science
and Technology, Saudi Arabia

Tom Trull,
Antarctic Climate & Ecosystem
Cooperative Research Centre,
Australia

*Correspondence:

Natasha A. Gafar
n.gafar.10@student.scu.edu.au

Specialty section:

This article was submitted to
Marine Biogeochemistry,
a section of the journal
Frontiers in Marine Science

Received: 25 October 2017

Accepted: 14 December 2017

Published: 04 January 2018

Citation:

Gafar NA, Eyre BD and Schulz KG
(2018) A Conceptual Model for
Projecting Coccolithophorid Growth,
Calcification and Photosynthetic
Carbon Fixation Rates in Response to
Global Ocean Change.
Front. Mar. Sci. 4:433.
doi: 10.3389/fmars.2017.00433

Temperature, light and carbonate chemistry all influence the growth, calcification and photosynthetic rates of coccolithophores to a similar degree. There have been multiple attempts to project the responses of coccolithophores to changes in carbonate chemistry, but the interaction with light and temperature remains elusive. Here we devise a simple conceptual model to derive a fit equation for coccolithophorid growth, photosynthetic and calcification rates in response to simultaneous changes in carbonate chemistry, temperature and light conditions. The fit equation is able to account for up to 88% of the variability in measured metabolic rates. Equation projections indicate that temperature, light and carbonate chemistry all have different modulating effects on both optimal growth conditions and the sensitivity of responses to extreme environmental conditions. Calculations suggest that a single extreme environmental condition (CO₂, temperature, light) will reduce maximum rates regardless of how optimal the other environmental conditions may be. Thus, while the response of coccolithophores to ocean change depends on multiple variables, the one which is least optimal will have the most impact on overall rates. Finally, responses to ocean change are usually reported in terms of cellular rates. However, changes in cellular rates can be a poor predictor for assessing changes in production at the community level. We therefore introduce a new metric, the calcium carbonate production potential (CCPP), which combines the independent effects of changes in growth rate and cellular calcium carbonate content to assess how environmental changes will impact coccolith production. Direct comparison of CO₂ impacts on cellular CaCO₃ production rates and CCPP shows that while the former is still at 45% of its pre-industrial capacity at 1,000 μatm, the latter is reduced to 10%.

Keywords: growth rate, photosynthesis, calcification, *Gephyrocapsa oceanica*, climate change, carbonate chemistry, temperature, light

1. INTRODUCTION

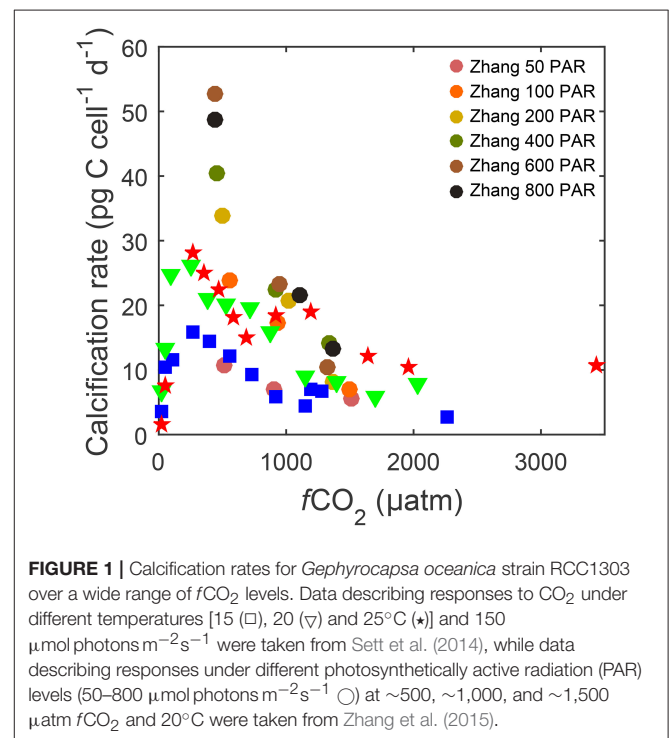
Coccolithophores are an abundant, ubiquitous component of marine phytoplankton assemblages (McIntyre and Bé, 1967; Charalampopoulou, 2011; Okada and Honjo, unpublished manuscript). As a functional group, coccolithophores have been influencing the Earth's biogeochemical element cycling for over 200 million years (Ridgwell, 2005; de Vargas et al., 2007). These organisms can contribute up to 20% of the total carbon production (calcification plus photosynthesis) in some ecosystems (Poulton et al., 2007, 2010), and up to 50% to the calcium carbonate (CaCO_3) content found in Holocene marine sediments (Broecker and Clark, 2009). Furthermore, several coccolithophore species also form extensive, dense blooms that cover up to 10,000 km^2 (Holligan et al., 1993a,b). Mass production of coccoliths by coccolithophores feeds-back to the marine carbon cycle by decreasing surface alkalinity and dissolved inorganic carbon in a 2:1 ratio, thus shifting carbonate chemistry toward CO_2 (Holligan et al., 1993a; Westbroek et al., 1993). Mass production of coccoliths may also enhance carbon sequestration in deep ocean waters by acting as ballast for organic carbon particles (Beaufort and Heussner, 1999; Armstrong et al., 2002). Finally it is hypothesized that DMSP production by coccolithophore blooms, in particular *Emiliania huxleyi*, may influence the Earth's albedo (Holligan et al., 1993a). As such, changes in coccolithophore abundance and productivity have the potential to significantly impact both the marine and global carbon cycles (Zondervan et al., 2001; Riebesell et al., 2009).

Since the Industrial Revolution in the late Eighteenth century, human activities started to significantly perturb the natural carbon cycle. Burning of fossil fuels, as well as wide scale deforestation have contributed to an increase in atmospheric partial pressures of carbon dioxide ($p\text{CO}_2$) from a pre-industrial level of $\sim 280 \mu\text{atm}$ to the current level of $\sim 400 \mu\text{atm}$ (IPCC, 2013a). Atmospheric CO_2 levels are projected to reach up to $985 \mu\text{atm}$ (RCP8.5 scenario) by the end of the century (Caldeira and Wickett, 2005; Orr et al., 2005; IPCC, 2013a). Under these conditions, ocean surface temperatures are projected to increase by as much as 4.8°C (IPCC's RCP8.5 scenario) (IPCC, 2013b). This increase in CO_2 and temperature is expected to have significant effects on ocean mixing and stratification which in turn will impact nutrient and light availability (Bopp et al., 2001; Rost and Riebesell, 2004; Sarmiento et al., 2004). In addition, rising atmospheric CO_2 levels are also bound to significantly change the ocean's carbonate chemistry.

An increased uptake of atmospheric CO_2 in the surface ocean will result in increased dissolved CO_2 , bicarbonate (HCO_3^-) and hydrogen ions (H^+)/decreased pH but also in decreased carbonate ion concentrations (CO_3^{2-}) (Doney et al., 2009; Schulz et al., 2009). These changes, often termed ocean acidification, are likely to have significant effects on coccolithophore physiology (growth, calcification and photosynthesis), which has important implications for coccolithophore related global biogeochemical processes (e.g., oceanic CO_2 uptake and sequestration) (Bopp et al., 2001; Sarmiento et al., 2004).

Previous studies (i.e., Bach et al., 2011; Sett et al., 2014; Bach et al., 2015), have established a unifying frame work where coccolithophore responses to carbonate chemistry can be described as a balance between the fertilizing effects of substrate (CO_2 and HCO_3^-) availability (Bach et al., 2011) and the inhibiting effects of hydrogen ions (H^+) (Bach et al., 2011, 2013). At one end of the scale, process-based numerical models describing intra-cellular inorganic carbon fluxes in response to changes in seawater carbonate chemistry and the resulting effects on coccolithophorid metabolic rates have been developed using this framework (Holtz et al., 2015a,b). On the other side of the complexity spectrum, there are simple fit equations based on this conceptual framework describing metabolic rates as being balanced by substrate availability, and inhibition by rising H^+ (Bach et al., 2011, 2015).

The downside of current equations however is that, unlike some numerical models, they lack the ability to describe responses to the interactive effects of other environmental variables, in particular temperature and light. For example at the same CO_2 level, calcification can vary from 10 to 54 pg C d^{-1} depending on light ($50\text{--}800 \mu\text{mol photons m}^{-2}\text{s}^{-1}$) and from 15 to 30 pg C d^{-1} depending on temperature ($15\text{--}25^\circ\text{C}$) (Figure 1). The influence of temperature and light on metabolic rates are as large as or even larger than the influence of CO_2 . A single analytical fit equation to fit measured response rates at various temperature, light and carbonate chemistry conditions would be useful to assess species specific sensitivities, optima and tipping points under future environmental conditions. Furthermore, comparing different species would allow exploration of the effects of ocean change on future coccolithophore community composition.



Here we develop a simple conceptual model for predicting coccolithophorid growth, photosynthesis and calcification in response to changes in temperature, light and carbonate chemistry. The majority of work on these effects comes from two species, *Emiliania huxleyi* and *Gephyrocapsa oceanica*. *E. huxleyi* has decoupled and coupled carbonate chemistry system data as well as temperature response data available for a single strain (i.e., Bach et al., 2011, 2013; Sett et al., 2014). However, there is no light response data for this same strain. Meanwhile for a single *G. oceanica* strain, temperature, light and coupled carbonate chemistry response data are available, but no decoupled data exists (Sett et al., 2014; Zhang et al., 2015). Decoupled carbonate chemistry data (changing CO₂ at constant pH) has been used to develop the concept of substrate stimulation and proton inhibition (Bach et al., 2011, 2013). However, it is not necessary to describe responses to ongoing ocean change in a coupled system. Hence it was decided that *G. oceanica* would be used as it had light, temperature and carbonate chemistry data available for the same strain. The resulting analytical equation was used to fit measured metabolic rates of the *G. oceanica* strain, to assess the interactive effects of temperature, light and carbonate chemistry on growth, calcification and photosynthesis. The equation was also used to test two additional concepts. In the first it was used to assess if comparable responses would be obtained from two, widely used, carbonate chemistry manipulation methods. In one method, total alkalinity (TA) was kept constant in the other dissolved inorganic carbon (DIC) was kept constant. In the second the equation was used to assess how changes in cellular calcification rates impact calcium carbonate production on the community level.

2. METHODS

2.1. Data Collection

Published studies by Sett et al. (2014) and Zhang et al. (2015) on the effects of changes in carbonate chemistry on a single strain of *Gephyrocapsa oceanica* RCC1303 were used to compile a uniform dataset containing: Specific growth rates μ (day⁻¹), particulate organic and inorganic carbon (POC and PIC) quotas (pg C cell⁻¹) and production rates (pg C day⁻¹), $f\text{CO}_2$ (μatm), $[\text{CO}_2]$ ($\mu\text{mol kg}^{-1}$), $[\text{HCO}_3^-]$ ($\mu\text{mol kg}^{-1}$), $[\text{CO}_3^{2-}]$ ($\mu\text{mol kg}^{-1}$), pH_T (on the total scale), total alkalinity/TA ($\mu\text{mol kg}^{-1}$), dissolved inorganic carbon/DIC ($\mu\text{mol kg}^{-1}$), photosynthetic active radiation/PAR ($\mu\text{mol photons m}^{-2}\text{s}^{-1}$) and temperature ($^{\circ}\text{C}$). Growth rates for all studies were based on specific growth rate μ (d⁻¹).

$$\mu = \frac{\ln(C_t) - \ln(C_0)}{d} \quad (1)$$

where C_t and C_0 are cell concentrations at the end and beginning of the experiment during exponential growth, respectively, and d is the duration of incubation in days. Calcification and photosynthetic rates were obtained by multiplying growth rates with cellular quotas of particulate inorganic or particulate organic carbon, respectively. Two studies were chosen as they utilized the same strain (RCC1303) and provided light (six levels)

and temperature (3 levels) interactions over a broad carbonate chemistry range (in total 54 data points). Two additional studies by Zondervan et al. (2001) and Rickaby et al. (2010) on two other *G. oceanica* strains PC7/1 and Pz3.1 were not included. Data were not included as they were providing no additional light, temperature or CO₂ coverage, but would increase unexplained variance due to strain-specific responses (compare Langer et al., 2009).

2.2. Carbonate Chemistry Standardization

Carbonate chemistry was standardized using CO2SYS (Lewis et al., 1998) and the stoichiometric equilibrium constants K_1 and K_2 for carbonic acid determined by Lueker et al. (2000), K_S for sulphuric acid determined by Dickson et al. (1990) and K_B for boric acid following Uppström (1974). Calculated pH is reported on the total scale. As input parameters temperature, salinity, phosphate concentrations and original (quality controlled) carbonate chemistry measurements (dissolved inorganic carbon/DIC and total alkalinity/TA) of the original studies were used. Any replicate values within a single treatment level were averaged prior to re-calculations (See Table S1 for the final corrected and standardized dataset).

2.3. Previous Efforts to Fit Coccolithophorid Performance

The first efforts to fit measured changes in coccolithophorid metabolic rates in response to changes in carbonate chemistry (Bach et al., 2011) were a modified Michaelis-Menten equation augmented by a negative sensitivity constant (s), with physiological rates solely a function of CO₂ fugacity ($f\text{CO}_2$)

$$V = \frac{X \times f\text{CO}_2}{Y + f\text{CO}_2} - s \times f\text{CO}_2 \quad (2)$$

where V denotes growth or organic and inorganic carbon fixation rates, X (pg C cell⁻¹ day⁻¹ or day⁻¹) and Y ($\mu\text{mol kg}^{-1}$) the theoretical maximum rate of the Michaelis-Menten term and the $f\text{CO}_2$ at which maximum rates are half-saturated, respectively, and s ($\mu\text{mol}^{-1} \text{kg}$) a negative linear term to account for the observed negative effects of increasing $f\text{CO}_2$.

This analytical equation was later modified and improved for fitting calcification rates in Bach et al. (2015). Although also a modified Michaelis-Menten equation, hydrogen ions (H⁺), rather than $f\text{CO}_2$, had been identified as the actual inhibiting factor influencing biological rates. Additionally, the substrate analog of $f\text{CO}_2$ was replaced with bicarbonate (HCO₃⁻) which is considered the primary substrate for calcification and photosynthesis (Rokitta and Rost, 2012; Kottmeier et al., 2014, 2016a). Therefore, rather than depending solely upon $f\text{CO}_2$, metabolic rates were now dependent upon the concentration of bicarbonate ions (HCO₃⁻), with the addition of two negative terms to account for the limiting and inhibiting effects of relatively low CO₂ and high hydrogen ion (H⁺) concentrations, respectively

$$V = \frac{a[\text{HCO}_3^-]}{b + [\text{HCO}_3^-]} - e^{-c[\text{CO}_2]} - d[\text{H}^+] \quad (3)$$

where a (dimensionless) and b (mol kg^{-1}) represent stimulation of metabolic rates by increasing $[\text{HCO}_3^-]$, c (kg mol^{-1}) parameterizes the indirect effects of CO_2 limitation on rates, and d (kg mol^{-1}) describes the linear negative effect of increasing $[\text{H}^+]$. The exponential term in the above equation represents a minimum requirement for CO_2 , with strong influence on observed rates at relatively low concentrations and negligible influence above a certain threshold. In the above analytical equations the fitting coefficients (X , Y , a , b , c , and d) will change depending on the temperature and light conditions. Considering that temperature and light have been observed to effect physiological responses to a similar degree as changing carbonate chemistry (Figure 1), developing fit equations able to account for the combined effects of temperature, light and carbonate chemistry would be necessary to project responses to future ocean conditions.

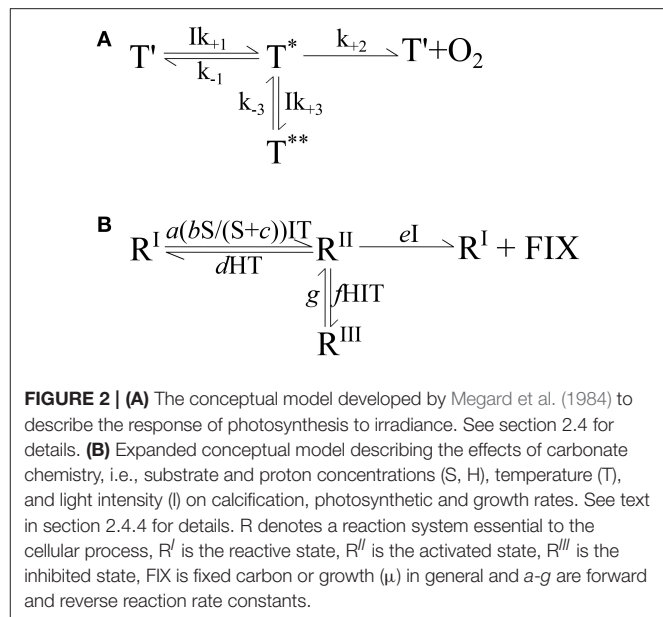
2.4. Development of a Conceptual Model of the Interactive Effects of Carbonate Chemistry, Temperature, and Light on Coccolithophorid Performance

The starting point for development of the conceptual model was Megard et al. (1984) and their equation on the response of photosynthesis to irradiance. Their pigment traps (T) were assumed to capture the light ultimately driving photosynthesis (compare Figure 2A). The traps have three states: a reactive state (T') able to capture light (I) at a rate $Ik_{+1}T'$, an activated state (T^*) able to catalyze photosynthesis to produce oxygen at a rate $k_{+2}T^*$, and an inhibited state (T^{**}) encountered when excess light is absorbed by an activated trap which occurs at a rate $Ik_{+3}T^*$. The trap is assumed to revert from the inhibited state at a constant rate $k_{-3}T^{**}$. The activated state (T^*) can also revert back to the reactive state (T') by a number of processes (i.e., fluorescence or heat) at a constant rate $k_{-1}T^*$. Using this physiological concept, they were able to reproduce both the limiting and inhibiting effects of light on photosynthesis.

In the following paragraphs we expand this simple conceptual model to include observed effects of changes in temperature and carbonate chemistry (i.e., substrate and inhibitor availability). We also expand the conceptual model to predict calcification and growth rates as well as photosynthetic rates.

2.4.1. Effects of Light on Cellular Processes

Photosynthesis, calcification and growth rates depend on light availability. photosynthetic rates increase with light availability up to a saturating point after which they begin to decline due to the damaging effects of light inhibition (Powles, 1984; Larsen, 2012). Similarly the rate of coccolithophore calcification has been observed to significantly increase with irradiance from low ($<50 \mu\text{mol photons m}^{-2}\text{s}^{-1}$) to saturating intensities ($>150 \mu\text{mol photons m}^{-2}\text{s}^{-1}$) (Nimer and Merrett, 1993; Feng et al., 2008), as well as growth rates between 50 and 800 $\mu\text{mol photons m}^{-2}\text{s}^{-1}$ (Zhang et al., 2015). In this experimental light range, inhibition of growth and calcification rates by high light is not as pronounced as for photosynthetic rates, but would eventually occur with increasing light intensity. Thus, it can be



concluded that the effects of light for all rates largely follow the non-linear stimulation-inhibition concept of Megard.

2.4.2. Effects of Temperature on Cellular Processes

Increasing temperature, accelerates coccolithophore metabolic rates up to an optimum level (i.e., Eppley, 1972; Helm et al., 2007). Beyond this level, with temperatures continuing to increase, metabolic rates start decreasing down to a point where metabolism can completely shut down (reviewed in Pörtner and Farrell, 2008; Larsen, 2012). This simple stimulation-inhibition observation of temperature is similar to that of light. As such, the effects of temperature are also captured by Megard's conceptual model.

2.4.3. Effects of Carbonate Chemistry on Cellular Processes

In an ocean acidification scenario (increasing CO_2 and decreasing pH) all rates increase to an optimum before declining again as conditions become more unfavorable (Bach et al., 2011, 2013). In a decoupled system (increasing CO_2 and constant pH) rates increase and then level off in a Michaelis-Menten fashion (Bach et al., 2011, 2013). These effects can be understood as stimulation by substrate ($\text{CO}_2 + \text{HCO}_3^-$) and inhibition by H^+ . How this will be incorporated into a conceptual model together with light and temperature will be discussed in the following sections.

2.4.4. Using a Single Conceptual Model for Growth, Calcification, and Photosynthesis

Both photosynthesis and calcification work in a similar way in that both are driven by substrate and enzyme/template interactions (i.e., RuBisCO with CO_2 in photosynthesis, and Ca^{2+} and HCO_3^- with with an organic template and polysaccharides in calcification) (Paasche, 2001; Farazdaghi, 2011). Although technically a substrate, Ca^{2+} can practically

be considered non-limiting as its concentrations in seawater are typically orders of magnitude higher than that of dissolved inorganic carbon. In fact Ca^{2+} has only been observed to limit calcification at un-naturally low concentrations (Herfort et al., 2004; Trimborn et al., 2007; von Dassow et al., 2012), so its availability is unlikely to affect reaction kinetics. As such, the same reaction system-substrate concept can be used for either calcification, photosynthesis or growth rates in general, the latter depending on photosynthetic performance.

An important assumption made for the conceptual model at this point is that the concentrations of the relevant carbonate chemistry species (H^+ , HCO_3^- , CO_2) inside the relevant cell compartments (i.e., chloroplast for photosynthesis and coccolith production vesicle for calcification) scale with bulk seawater concentrations outside the cell. That means that decreasing seawater concentrations result in a respective decrease inside the cell and vice-versa (i.e., Coleman and Colman, 1981). Evidence for a connection of the inorganic carbon pool in seawater and inside phytoplankton cells stems from conceptual models relating supply and demand to observed stable carbon isotope fractionation (e.g., Sharkey and Berry, 1985; Laws et al., 1995; Burkhardt et al., 1999; Keller and Morel, 1999). While a multitude of studies have shown that phytoplankton species actively take up both CO_2 and HCO_3^- (e.g., Burkhardt et al., 2001; Rost et al., 2003), the internal pools are significantly influenced by passive diffusion of CO_2 into and out of the cell which theoretically scales linearly with extracellular CO_2 concentrations (e.g., Schulz et al., 2007 and references therein). Concerning proton concentrations, there is experimental evidence that bulk seawater pH can influence internal concentrations in a linear fashion (Suffrian et al., 2011), probably mediated by voltage-gated H^+ channels (Taylor et al., 2011). Hence, and given the fact that there are no direct measurements on the exact magnitude of external in relation to internal changes, a linear relationship was assumed.

The next step was to decide how to implement the effects of light, temperature and carbonate chemistry within the conceptual model (See **Figure 2B**). The effects of light and temperature are very simple with both a stimulating and an inhibiting effect on rates. Both light and temperature could be said to affect all reaction steps. However, it was found that applying temperature and light dependency to all reactions resulted in canceling out of terms and that the best compromise for light and temperature fits required a separation of temperature and light on at least one reaction step in the model. To implement the effects of carbonate chemistry into the model, CO_2 and HCO_3^- were combined and defined as substrate (S). While, the proportion of CO_2 and HCO_3^- utilized by growth, photosynthesis and calcification strongly depends upon carbonate chemistry conditions, for the sake of keeping the concept simple, it was assumed that all rates depended upon the combination of CO_2 and HCO_3^- and had no preference for one or the other (Kottmeier et al., 2014). It should be noted that, owing to its higher concentrations, this assumption gives more weight to changes in HCO_3^- . The stimulating effects of substrate availability on rates can then be described as a Michaelis-Menten saturation curve (Bach et al., 2011). The inhibiting effects of rising H^+

are slightly more complicated in that they are balanced, to a degree, by the positive effects of rising substrate concentrations (Bach et al., 2011). Because of this, two terms were required to provide an effective representation of H^+ effects across the whole CO_2 range. As carbonate chemistry is dependant on temperature, all reactions with carbonate chemistry dependencies also had temperature dependencies. Finally, it was found that applying temperature, light and carbonate chemistry dependencies to both forward and reverse reactions for inhibition resulted in a canceling out of terms and, as such, an insensitivity of inhibition to environmental conditions. Because of this, it was decided that the reverse reaction for inhibition would be assumed to be independent of environmental conditions.

In this conceptual model, the transition of the reactive (R^I) to activated (R^{II}) state follows a Michaelis-Menten substrate (S) kinetic, stimulated by light (I) and temperature (T), at a rate $a(bS/(S+c))ITR^I$. The activated state (R^{II}) may transition back to the reactive state (R^I), depending on the proton concentration (H) and temperature, at a rate $dHTR^{II}$. Furthermore the activated state can also transition to an inhibited state (R^{III}) by light, temperature and proton concentrations at a rate $fHITR^{II}$. The reversal back to the activated state (R^{II}) is at a rate gR^{III} , insensitive to environmental conditions (similar to Megard et al., 1984). Finally, the activated state can catalyze a reaction (photosynthesis, calcification, or growth in general) producing fixed carbon (FIX), and transition back to the reactive state (R^I) in a single step at a rate eIR^{II} , depending upon light.

With the sum of states in this reaction system being constant, i.e., $(R) = R^I + R^{II} + R^{III}$, the change in each of these three states with time can be expressed by the following three differential equations:

$$\frac{dR^I}{dt} = (dHT + eI)R^{II} - a\frac{bS}{S+c}ITR^I \quad (4)$$

$$\frac{dR^{II}}{dt} = a\frac{bS}{S+c}ITR^I + gR^{III} - (dHT + eI + fHIT)R^{II} \quad (5)$$

$$\frac{dR^{III}}{dt} = fHITR^{II} - gR^{III} \quad (6)$$

This set of differential equations was solved analytically for steady state conditions, i.e., assuming no change in each of the rates with with time, giving:

$$R^{II} = \frac{RSIT}{k_2HT + k_3SHT + k_4I + k_5SI + SIT + k_6SHI^2T^2} \quad (7)$$

where, $k_2 = dc/ab$, $k_3 = d/ab$, $k_4 = ce/ab$, $k_5 = e/ab$, and $k_6 = f/g$. The specific metabolic rate of photosynthesis, calcification or growth based on this equation is $MR = e \times R^{II}$ and the theoretical maximum rate of photosynthesis, calcification or growth, $k_1 = e \times R$, would occur if the reaction system would be solely in its active state, i.e., where $R = R^{II}$. Based on this, metabolic rates (MR) of photosynthesis, calcification and growth are

$$MR(T,I,S,H) = \frac{k_1SIT}{k_2HT + k_3SHT + k_4I + k_5SI + SIT + k_6SHI^2T^2} \quad (8)$$

2.4.5. Simplified Equations

Equation (Equation 8) can fit responses to changes in temperature, light and carbonate chemistry at the same time. For situations where only one environmental variable (temperature, light, carbonate chemistry) is variable, with the other two remaining constant, the model can be simplified to:

$$MR(S,H) = \frac{s_1 S}{s_2 H + s_3 S H + s_4 + s_5 S} \quad (9)$$

for describing carbonate chemistry (S, H) responses at constant light intensity and temperature,

$$MR(I) = \frac{i_1 I}{i_2 + i_3 I + i_4 I^2} \quad (10)$$

for light (I) responses at constant carbonate chemistry and temperature, and

$$MR(T) = \frac{t_1 T}{t_2 + t_3 T + t_4 T^2} \quad (11)$$

for temperature responses (T) at constant carbonate chemistry and light intensity, with s, i and t denoting respective fit parameters (Table 1).

2.5. Fitting Procedure

Equation (8) was fitted to measured *Gephyrocapsa oceanica* metabolic rates from Sett et al. (2014) and Zhang et al. (2015) using a non-linear regression procedure with the MATLAB function `nlinfit`, at corresponding HCO_3^- , CO_2 and H^+ (total scale) concentrations, light availability (I) and incubation temperature (T) as input parameters. Given the order of magnitude differences in fit coefficients, starting conditions were scaled by suitable multipliers for fitting purposes. Data were not weighted and were assumed to have equal uncertainties.

2.6. Temperature and Light Transformation

To reduce skew and allow for rate inhibition below and beyond certain temperature and light conditions, both temperature and light data were transformed. To reduce skew in the light data, a square root transform $I = \sqrt{\text{PFD}}$ was applied, where PFD = photon flux density of PAR (photosynthetic active radiation). *G. oceanica* will grow across a relatively broad range of temperatures with cultures failing to grow at and below 9°C and above 30°C (Rhodes et al., 1995; Buitenhuis et al., 2008; Larsen, 2012). Upper and lower limits for growth were included with the general transform of $T = (T_t - 9) \times (33 - T_t)$, where T_t is the temperature of each treatment. In order to accurately express the sharp onset of temperature inhibition in this species, the transform was further modified with a square root transform to give $T = (T_t - 9) \times \sqrt{(33 - T_t)}$. The temperature transform was compared with the Norberg thermal optimum envelope model (Norberg, 2004)

$$\text{Growth}(Z, T, w) = \left[1 - \left(\frac{T - Z}{w} \right)^2 \right] a e^{0.0633T} \quad (12)$$

TABLE 1 | Units for the fit coefficients of Equations (9–11).

Parameter	Equation 9	Equation 10	Equation 11
s_1, i_1, t_1		pg C cell ⁻¹ day ⁻¹ or day ⁻¹	
s_2, i_2, t_2	Dimensionless	μmol photons m ⁻² s ⁻¹	°C
s_3, i_3, t_3	Kg mol ⁻¹	Dimensionless	Dimensionless
s_4, i_4, t_4	Mol kg ⁻¹	μmol photons ⁻¹ m ² s	°C ⁻¹
s_5	Dimensionless	–	–

Note that for calcification and photosynthetic rates the unit of s_1, i_1, t_1 is pg C cell⁻¹ day⁻¹ and for growth rates day⁻¹.

with optimum (envelope) temperature set to $Z = 21$, the thermal window to $w = 12$ and using a scaling factor $a = 0.31$ to account for the fact that individual species do have maximum rates below the original Eppley curve. The shape of both fits was in good agreement [data not shown, but the reader is referred to Figure 2B in Norberg (2004)].

2.7. Equation Fit and Working Limits

The ability of the fit to describe the data in terms of carbonate chemistry, temperature and light was then examined. This initial evaluation focused on assessing if physiological features such as limitation and inhibition were present, as well as how much variability the equation explained. Following these tests, the limits of Equation (8) and its fit coefficients (Table 2) in terms of projecting responses outside of the current data range were tested. In the first test all rates were calculated at seven distinct light intensities (10, 50, 100, 200, 800, 1,000, 2,000 μmol photons m⁻²s⁻¹) over a DIC range of 1,200–3,000 μmol kg⁻¹ at constant TA of 2,350 μmol kg⁻¹ ($f\text{CO}_2$ down to 2 μatm and up to 5,000 μatm) and a temperature range of 9–33°C. In the second test rates were calculated at seven distinct temperatures (10, 12, 16, 20, 24, 28, 32°C) over a DIC range of 1,200–3,000 μmol kg⁻¹ at constant TA of 2,350 μmol kg⁻¹ ($f\text{CO}_2$ down to 2 μatm and up to 5,000 μatm) and light intensities of 10–2,500 μmol photons m⁻²s⁻¹. In the final test rates were calculated at six distinct $f\text{CO}_2$ levels (50, 200, 400, 1,000, 2,000, 3,000 μatm) over a temperature range of 9–33°C and light intensities between 10 and 2,500 μmol photons m⁻²s⁻¹. The results of all tests were visualized using contour plots. These plots were then used to define environmental working limits for equation 8 and its fit coefficients (Table 2).

2.8. Interaction of Temperature, Light and Carbonate Chemistry in Modulating Physiological Rates

Optimum CO_2 , light and temperature conditions, maximum rates (V_{max}) and CO_2 , temperature and light conditions at which rates are half-saturated or half-inhibited ($K_{\frac{1}{2}\text{sat}}$ and $K_{\frac{1}{2}\text{inhib}}$ respectively) were calculated and assessed for photosynthetic, calcification and growth rates using Equation (8) and the individual fit coefficients (Table 2).

TABLE 2 | Fit coefficients (k_1 , k_2 , k_3 , k_4 , k_5 , k_6), R^2 , p -values, F -values and degrees of freedom obtained from fit Equation (8) for calcification ($\text{pg C cell}^{-1} \text{d}^{-1}$), photosynthesis ($\text{pg C cell}^{-1} \text{d}^{-1}$) and growth rate (d^{-1}) fits to all data of Sett et al. (2014) and Zhang et al. (2015).

	Calcification	Photosynthesis	Growth
k_1 ($\text{pg C cell}^{-1} \text{day}^{-1}$ or day^{-1})	-9.01	-4.02	-0.64
k_2 ($\mu\text{mol photons m}^{-2}\text{s}^{-1}$)	-1.68E+06	-2.77E+06	8.22E+05
k_3 (kg mol^{-1} $\mu\text{mol photons m}^{-2}\text{s}^{-1}$)	3.05E+08	1.08E+09	-6.81E+08
k_4 ($\text{mol kg}^{-1} \text{ }^\circ\text{C}$)	-7.87E-02	-6.23E-02	-9.10E-02
k_5 ($^\circ\text{C}$)	10.46	-0.49	-6.17
k_6 ($\text{kg mol}^{-1} \mu\text{mol photons}^{-1}$ $\text{m}^2\text{s} \text{ }^\circ\text{C}^{-1}$)	-1.72E+04	-1.34E+04	-1.05E+04
R^2	0.8843	0.8512	0.8329
(p -value)	(<0.001)	(<0.001)	(<0.001)
F -value (degrees of freedom)	399 (52)	306 (52)	260 (52)

Note that for calcification and photosynthetic rates the unit of k_1 is $\text{pg C cell}^{-1} \text{day}^{-1}$ and for growth rates day^{-1} .

2.9. Coupled and Decoupled Carbonate Systems

In experimentally decoupled carbonate systems DIC concentrations increase while $[\text{H}^+]$ remains constant (Bach et al., 2013). This results in a saturation curve response with no H^+ inhibition. In coupled systems DIC and H^+ concentrations increase together resulting in an optimum curve response (Sett et al., 2014). The fit equation was designed to fit responses to both coupled and decoupled carbonate chemistry. However, no decoupled data currently exists for *G. oceanica*. In order to test if Equation (8) could describe responses for coupled and decoupled carbonate chemistry we fitted the equation to data on coupled and decoupled *E. huxleyi* experiments as in Bach et al. (2015). All data was first standardized following procedures described in section 2.2. The resulting fit coefficients were used to create a contour plot describing the effect of coupled (constant TA) and decoupled (varying TA) carbonate chemistry on projected calcification rates of *E. huxleyi*.

2.10. TA vs. DIC Manipulation

The two main forms of carbonate chemistry manipulation in experimental incubations are changing DIC at constant TA (DIC manipulation = CO_2 gas bubbling, combined additions of Na_2CO_3 and acid, or additions of CO_2 enriched seawater), and changing TA at constant DIC (TA manipulation = acid/base addition) in a closed system. These two approaches typically produce relatively comparable changes in carbonate chemistry. To examine potential effects of the two manipulation methods on measured metabolic rates, two scenarios were devised at constant light of $150 \mu\text{mol photons m}^{-2}\text{s}^{-1}$ and a temperature of 20°C . In one TA was set to a constant concentration of $2,350 \mu\text{mol kg}^{-1}$ and DIC was varied to produce a CO_2 range of $50\text{--}3,000 \mu\text{atm}$. In the other DIC was set to a constant concentration of $2,069 \mu\text{mol kg}^{-1}$ and TA was varied to produce a CO_2 range of $50\text{--}3,000 \mu\text{atm}$. That way both scenarios have exactly the same carbonate chemistry at $400 \mu\text{atm}$ ($\text{TA} = 2,350 \mu\text{mol kg}^{-1}$

and $\text{DIC} = 2,082 \mu\text{mol kg}^{-1}$) (Figure 3). Calculated H^+ , HCO_3^- and CO_2 (using K_1 and K_2 from Lueker et al., 2000) of both scenarios were then used to project physiological rates using Equation (8) (at a constant light of $150 \mu\text{mol photons m}^{-2}\text{s}^{-1}$ and temperature of 20°C) and fit coefficients in Table 2.

2.11. CaCO_3 Production Potential

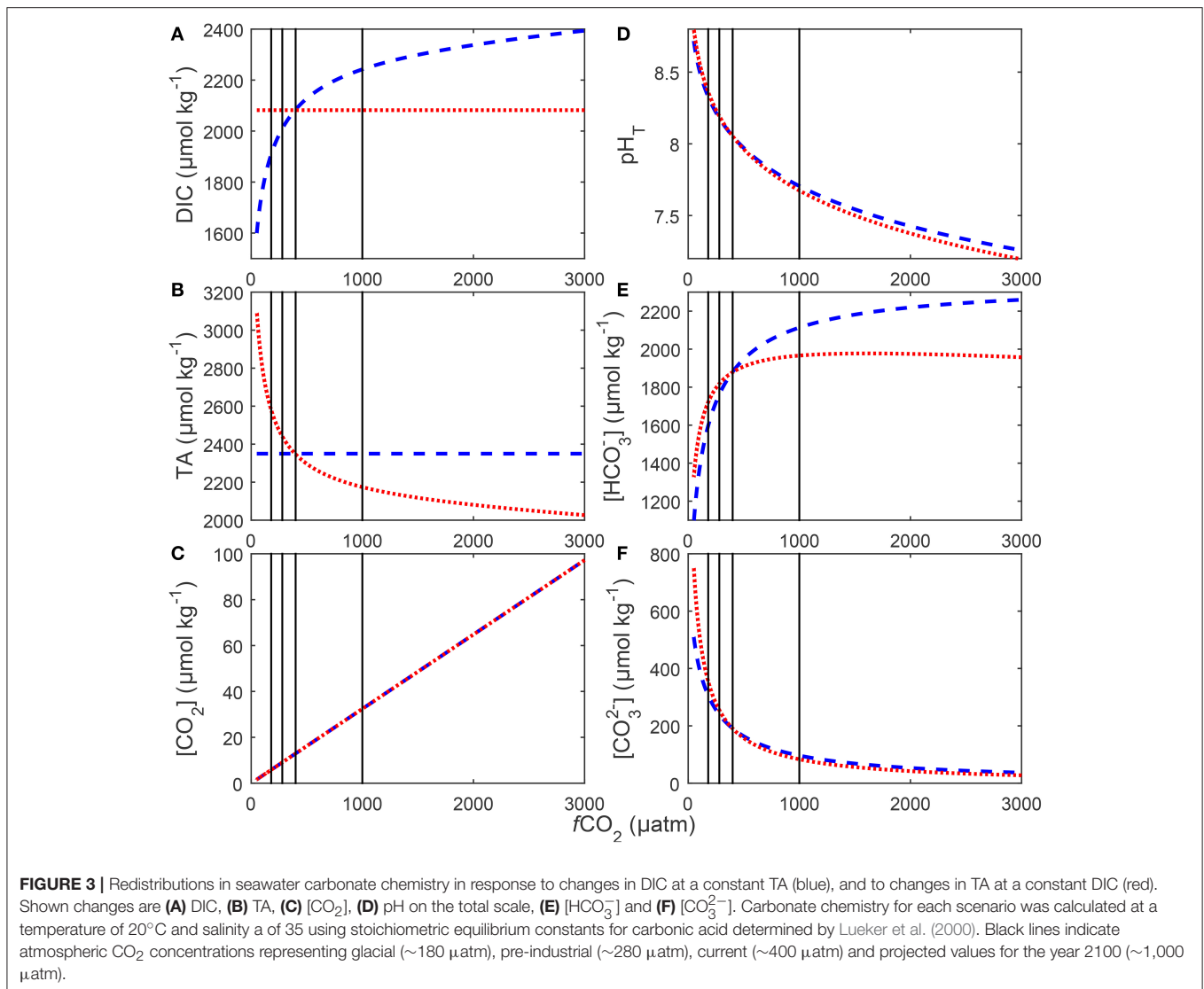
The response of coccolithophores to ocean change is typically measured using cellular production rates. However, in unicellular, asexually dividing organisms cellular production rates are affected by cellular quotas and cellular division rates. As such the same metabolic rate can be observed for different combinations of cellular quotas and growth rates. For instance, the same cellular calcification rate of $18 \text{pg C cell}^{-1} \text{day}^{-1}$ would be observed for a cell with a growth rate of 0.9d^{-1} and a CaCO_3 quota of 20pg C cell^{-1} , and a growth rate of 1d^{-1} and a CaCO_3 quota of 18pg C cell^{-1} . To examine how these cellular differences translate to the community level we extrapolated changes in the above communities over seven days, assessing their production potential. Using a known starting cell count and assuming constant exponential growth, the cellular standing stock can be calculated for each community for each day. The corresponding CaCO_3 production of these communities for each day can then be calculated by multiplying daily cellular standing stocks with cellular CaCO_3 quotas. The CaCO_3 production potential (CCPP) is then the amount of CaCO_3 produced within a week of growth. Finally, the cellular CO_2 response (pg C cell^{-1}) can be directly compared to those on the community level (pg C produced after 7 days) by normalizing each of them to respective values at, for instance, pre-industrial levels of $280 \mu\text{atm}$.

3. RESULTS

3.1. Equation Fit and Working Limits

Equation (8) with its coefficients was able to explain up to 88% of the variability in measured metabolic rates (compare Table 2) across a relatively broad range of carbonate chemistry ($25\text{--}3,500 \mu\text{atm}$), light ($50\text{--}800 \mu\text{mol photons m}^{-2}\text{s}^{-1}$) and temperature ($15\text{--}25^\circ\text{C}$) conditions. Furthermore, it was able to capture known physiological features like the limitation, stimulation and inhibition of rates by different light (Figure 4) and temperature conditions (data not shown). Equation (8) was also able to describe the effects of substrate limitation and stimulation and hydrogen ion (H^+) inhibition on metabolic rates (Figure 5).

Projecting Equation (8) beyond the range of the input data (i.e., $15 < T(^\circ\text{C}) > 25$, $20 < f\text{CO}_2(\mu\text{atm}) > 3,500$, $50 < I(\text{PAR}) > 800$), some limitations became evident at more extreme environmental conditions especially when in combination. While there were reasonable projections for most temperature, $f\text{CO}_2$ and light conditions (Figure 6A), both light and CO_2 inhibition were no longer observed for photosynthesis or growth rates at temperatures below 12°C and for calcification rates below 11°C (Figure 6C). Similarly, at $f\text{CO}_2$ levels above $2,000 \mu\text{atm}$ for calcification and photosynthesis and above $3,000 \mu\text{atm}$ for growth, rates were slightly overestimated at combined high temperature-light conditions owing to the appearance of a second temperature optimum (Figure 6B). In addition, estimates



for growth rates did not display light limitation at $f\text{CO}_2$ levels below 100 μatm . As a result, photosynthetic rates were overestimated at low $f\text{CO}_2$ levels. In summary, the working range for the equation is limited to temperatures above 12°C for photosynthetic and growth rates and 11°C for calcification rates, $f\text{CO}_2$ levels below 2,000 μatm for calcification and photosynthetic rates, and $f\text{CO}_2$ levels of 100–3,000 μatm for growth rates.

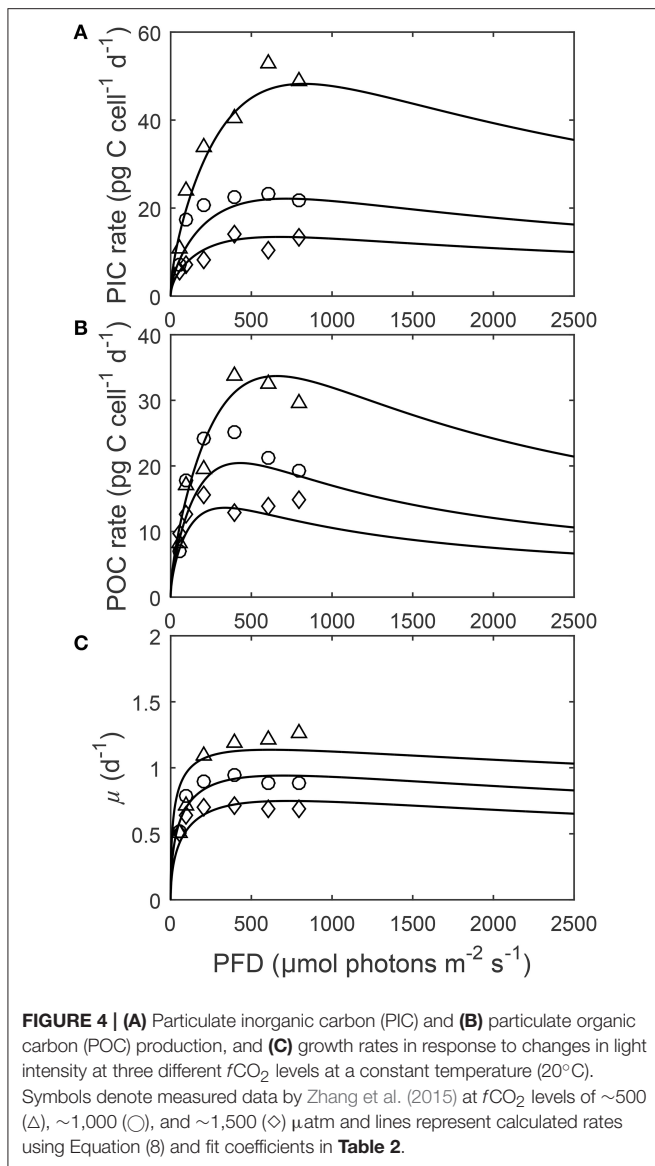
3.2. Interaction of Temperature, Light and Carbonate Chemistry in Modulating Physiological Rates

3.2.1. Light Responses

Depending upon the $f\text{CO}_2$ level, increasing light from 50 to 800 $\mu\text{mol photons m}^{-2}\text{s}^{-1}$ increased calcification rates 230%, photosynthetic rates 240% and growth rates 21% (Figure 4). The effect of $f\text{CO}_2$ on metabolic rates was strongest between 500 and 800 $\mu\text{mol photons m}^{-2}\text{s}^{-1}$ and decreased

with decreasing light availability (Figure 4). Increasing $f\text{CO}_2$ lowered light requirements for photosynthesis and calcification but increased light requirements for growth (Figure 4, Table 3). Optimum light levels were lowest for photosynthesis (338–657 $\mu\text{mol photons m}^{-2}\text{s}^{-1}$), moderate for growth (614–735 $\mu\text{mol photons m}^{-2}\text{s}^{-1}$), and highest for calcification (674–825 $\mu\text{mol photons m}^{-2}\text{s}^{-1}$) (Figure 4, Table 3).

Growth had the lowest light requirements to exceed half maximum rates ($K_{\frac{1}{2}\text{PAR}}^{\text{sat}}$) at 12.9–38.3 $\mu\text{mol photons m}^{-2}\text{s}^{-1}$, with photosynthesis requiring 47.6–115.2 $\mu\text{mol photons m}^{-2}\text{s}^{-1}$, and calcification requiring 76.7–134.7 $\mu\text{mol photons m}^{-2}\text{s}^{-1}$ (Figure 4, Table 3). Light requirements to exceed half maximum rates ($K_{\frac{1}{2}\text{PAR}}^{\text{sat}}$) decreased with increasing $f\text{CO}_2$ for calcification and photosynthesis but increased with increasing $f\text{CO}_2$ for growth (Table 3). Light inhibition for this species was not pronounced within the measured data range of 50–800 $\mu\text{mol photons m}^{-2}\text{s}^{-1}$. As a result, rates calculated by the fit did not decrease below half of maximum ($K_{\frac{1}{2}\text{PAR}}^{\text{inhib}}$) within our working light range of 0–2,500 $\mu\text{mol photons m}^{-2}\text{s}^{-1}$.

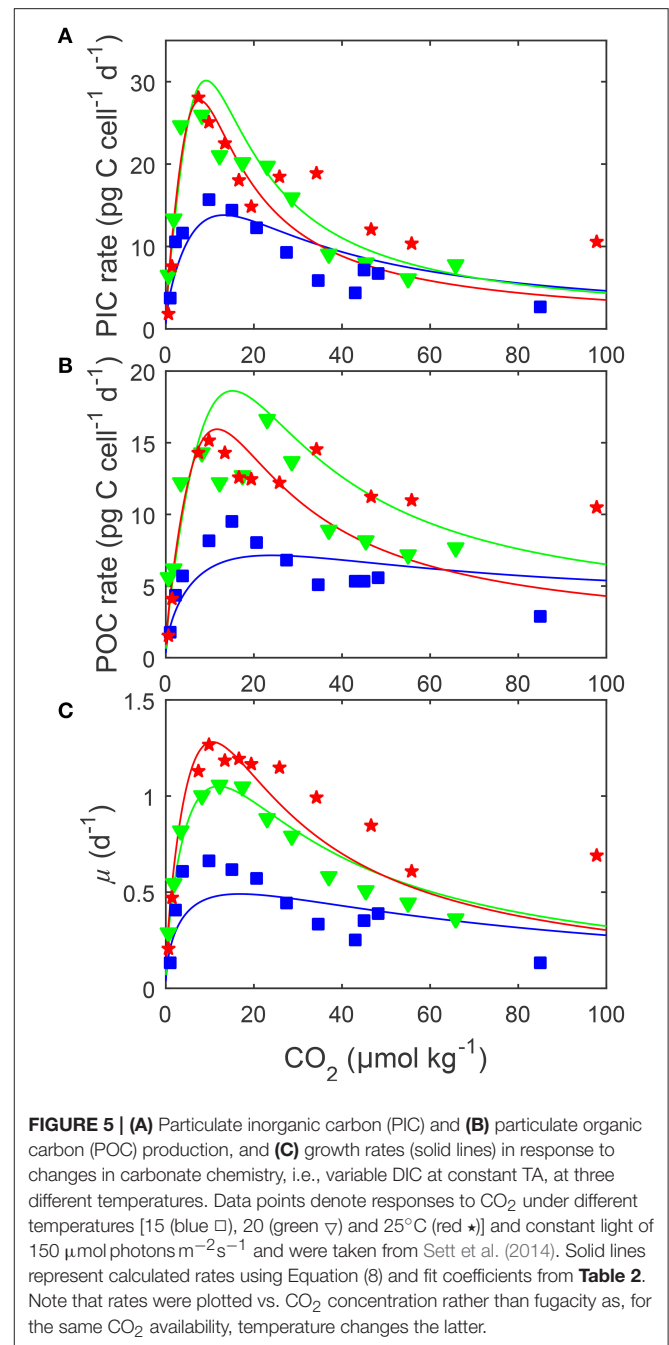


3.2.2. Temperature Responses

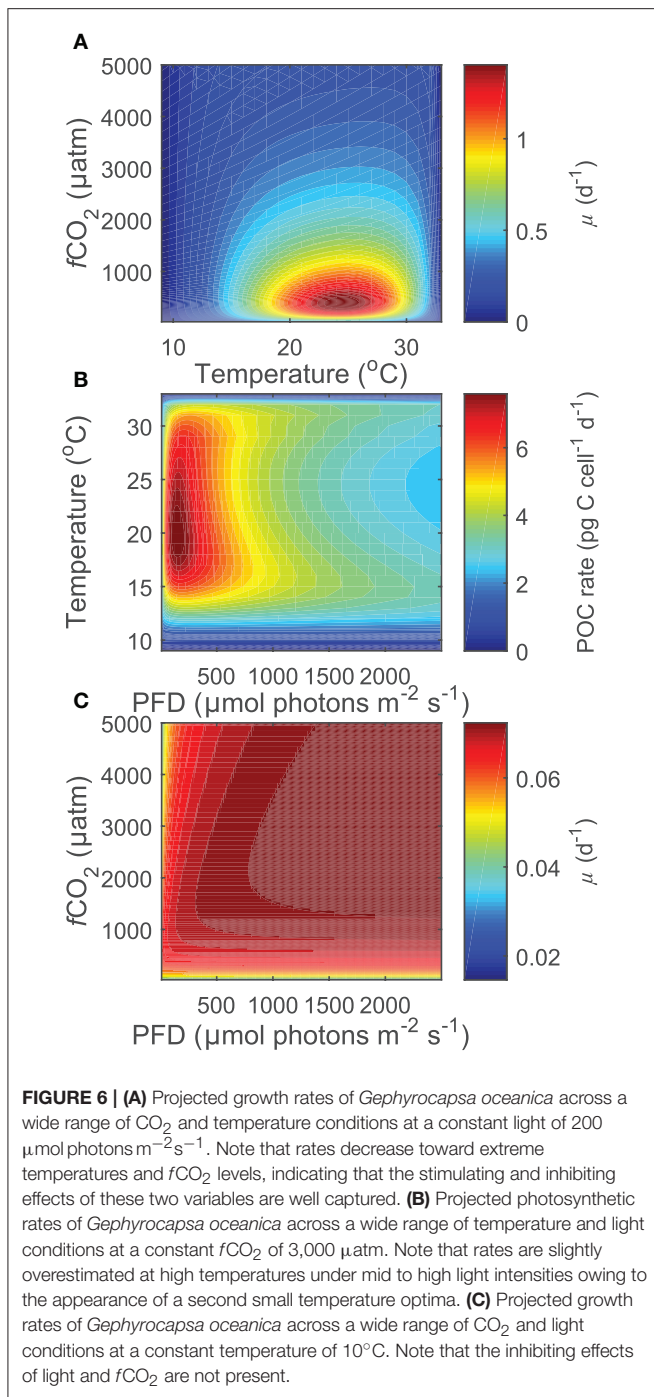
Depending on the CO_2 level, increasing temperature from 15 to 25°C more than doubled all metabolic rates (**Figure 5**). The effect of temperature on metabolic rates was highest in the optimal CO_2 range between 5 and $30 \mu\text{mol kg}^{-1}$ and decreased toward more extreme CO_2 concentrations (**Figure 5**). Photosynthesis and calcification had maximum rates of 19.0 and $28.4 \text{ (pg C d}^{-1}\text{)}$ at temperatures of approximately 23.0°C while growth rates had maximum rates of $1.31 \text{ (d}^{-1}\text{)}$ at temperatures of approximately 24.5°C (**Table 4**). Temperatures at which rates were half saturated ($K_{\frac{1}{2}\text{Temp sat}}$) and half inhibited ($K_{\frac{1}{2}\text{Temp inh}}$) were between $15\text{--}17^\circ\text{C}$ and $29\text{--}31^\circ\text{C}$, respectively, for all rates (**Table 4**).

3.2.3. Effects of Carbonate Chemistry on Cellular Processes

By including terms for carbonate chemistry (i.e., S and H) Equation (8) was able to describe the limitation and stimulation



of metabolic rates at sub-saturating substrate concentrations, as well as the inhibition of rates by increasing H^+ concentrations (**Figure 5**). By including terms for temperature, Equation (8) was also able to describe how the effects of limitation, stimulation and inhibition were modulated by temperature (**Figure 5**). Optimum CO_2 concentrations required for growth, photosynthesis and calcification showed a slight tendency toward lower CO_2 at higher temperatures (**Table 5**, **Figure 5**). Optimum CO_2 concentrations also varied slightly between the different processes with optimum calcification observed at $10.0 \pm 2.8 \mu\text{mol kg}^{-1}$, optimum photosynthesis at $16.9 \pm 6.4 \mu\text{mol kg}^{-1}$,



and optimum growth rates at $13.1 \pm 3.3 \mu\text{mol kg}^{-1}$ (Table 5). The CO₂ concentrations at which rates were half saturated ($K_{\frac{1}{2}\text{CO}_2}^{\text{sat}}$) displayed very little change with varying temperature (Table 5). The CO₂ concentration at which rates were half-inhibited by increasing H⁺ levels ($K_{\frac{1}{2}\text{CO}_2}^{\text{inhib}}$) were highest at lower temperatures, indicative of a lower sensitivity (Table 5, Figure 5). Inhibition by increasing H⁺ concentrations also varied between the processes with $K_{\frac{1}{2}\text{CO}_2}^{\text{inhib}}$ observed at lower CO₂ concentrations for calcification, than for photosynthetic or growth rates (Table 5).

TABLE 3 | Calculated optimum light intensities, maximum rates (V_{max}) and light $K_{\frac{1}{2}}^{\text{PAR}}$ values at constant temperature (20°C) and carbonate chemistry (500, 1,000, and 1,500 μatm) using Equation (8) and fit coefficients from Table 2.

Light	500 μatm	1,000 μatm	1,500 μatm
Optima (μmol photons m⁻²s⁻¹)			
Calcification	825	718	674
Photosynthesis	657	431	338
Growth	614	700	735
V_{max} (pg C cell⁻¹ d⁻¹ or d⁻¹)			
Calcification	48.2	22.1	13.4
Photosynthesis	33.7	20.4	13.6
Growth	1.14	0.94	0.75
K₂^{PAR} sat (μmol photons m⁻² s⁻¹)			
Calcification	135	95.0	76.7
Photosynthesis	115	69.5	47.6
Growth	12.9	29.3	38.3

$K_{\frac{1}{2}\text{PAR}}^{\text{sat}}$ is the light intensity below which the rate drops below half its maximum by light limitation.

TABLE 4 | Calculated optimum temperatures, maximum rates (V_{max}) and $K_{\frac{1}{2}}^{\text{Temp}}$ temperature values at constant carbonate chemistry (400 μatm) and light (150 μmol photons m⁻² s⁻¹) using Equation (8) and fit coefficients from Table 2.

Temperature	
Optima (°C)	
Calcification	23.1
Photosynthesis	23.0
Growth	24.5
V_{max} (pg C cell⁻¹ d⁻¹ or d⁻¹)	
Calcification	28.4
Photosynthesis	19.0
Growth	1.31
K₂^{Temp} inhib (°C)	
Calcification	30.4
Photosynthesis	29.3
Growth rate	30.6
K₂^{Temp} sat (°C)	
Calcification	15.5
Photosynthesis	16.8
Growth	16.7

$K_{\frac{1}{2}\text{Temp}}^{\text{sat}}$ and is the temperature below which the rate drops below half its maximum by low temperature inhibition. $K_{\frac{1}{2}\text{Temp}}^{\text{inhib}}$ is the temperature beyond which the rate drops below half its maximum by high temperature inhibition.

3.3. Coupled and Decoupled Carbonate Systems

Fitting Equation (8) to cellular calcification rates of *E. huxleyi* (Bach et al., 2013) demonstrates the ability of the conceptual model to capture both coupled (as in the case for the *G. oceanica* data sets by Sett et al., 2014; Zhang et al., 2015) and decoupled (Bach et al., 2013) carbonate chemistry conditions. For the case of an ocean acidification scenario, i.e., coupled carbonate chemistry

TABLE 5 | Calculated optimum CO₂ concentrations, maximum rates (V_{max}) and CO₂ K_{1/2} values at 15, 20, and 25°C, 150 μmol photons m⁻²s⁻¹ and variable CO₂ using Equation (8) and fit coefficients from **Table 2**.

CO ₂	15°C	20°C	25°C
Optima μmol kg⁻¹			
Calcification	13.2	9.15	7.74
Photosynthesis	24.0	15.1	11.7
Growth	16.8	11.9	10.6
V_{max} (pg C cell⁻¹ d⁻¹ or d⁻¹)			
Calcification	13.8	30.1	27.7
Photosynthesis	7.14	18.6	15.9
Growth	0.49	1.05	1.28
K_{1/2}CO₂ inhib (μmol kg⁻¹)			
Calcification	60.9	29.3	25.4
Photosynthesis	>130	60.6	45.8
Growth	119	57.0	44.6
K_{1/2}CO₂ sat (μmol kg⁻¹)			
Calcification	2.22	2.41	1.96
Photosynthesis	2.63	3.46	2.55
Growth	1.43	1.80	1.90

K_{1/2}CO₂ inhib is the CO₂ concentration beyond which the rate drops below half its maximum rate because of proton inhibition (in a coupled carbonate system). *K_{1/2}CO₂ sat* is the CO₂ concentration below which the rate drops below half its maximum by low substrate availability. Note that the *K_{1/2}CO₂ inhib* for photosynthesis at 15°C exceeds the CO₂ working range for the equation, as a result it was reported as >130 μmol kg⁻¹.

conditions at increasing *f*CO₂ and constant TA, rates are calculated to be low at low *f*CO₂-low [H⁺] conditions, optimal at intermediate *f*CO₂-low [H⁺] conditions, and low again at high *f*CO₂-high [H⁺] conditions (**Figure 7**, TA constant line). In the decoupled carbonate chemistry scenario, i.e., increasing *f*CO₂ at constant [H⁺], rates are calculated to be low at low *f*CO₂ conditions, to increase to an optimal point under intermediate *f*CO₂ conditions, and to remain stable with further increases in *f*CO₂ (**Figure 7**, pH constant line). In both cases the calculated pattern of response agreed with the measured response of calcification rates to coupled and decoupled carbonate chemistry manipulations (**Figure 7**).

3.4. DIC vs. TA Manipulation

Calculated physiological rates at constant DIC were consistently lower than at constant TA at *f*CO₂ levels above 500 μatm (**Figure 8**). Within this range, rates decreased to a similar magnitude with rising *f*CO₂ in both manipulations. As a result a relatively constant offset of overall rates was maintained between the manipulation methods above 500 μatm (**Figure 8**). Below 500 μatm both methods displayed an optimum curve response to rising *f*CO₂. However, optima were shifted toward lower CO₂ levels in the constant DIC manipulations versus the constant TA ones (**Figure 8**). Calcification and photosynthesis displayed significantly higher V_{max} and growth a slightly higher V_{max} in the DIC constant treatment relative to the TA constant one (**Figure 8**).

There were no significant differences in [CO₂], pH, and [CO₃²⁻] calculated between the two manipulation methods (compare **Figure 3**). Concentrations in HCO₃⁻ were slightly higher in the TA constant manipulation below 400 μatm and significantly higher in the DIC constant manipulation above 400 μatm (**Figure 3**).

3.5. CaCO₃ Production Potential (CCPP)

A single cell dividing at a rate μ = 1 d⁻¹ will grow to a community of 1,097 cells within one week. In comparison a single cell dividing at a rate μ = 0.9 d⁻¹ will only grow to a community of 545 cells in a week (**Figure 9A**). At the same cellular calcification rate of 18 pg PIC cell⁻¹ day⁻¹, the community dividing at μ = 1 d⁻¹ has a CaCO₃ production potential (CCPP) of 19.7 ng PIC while the one growing at 0.9 d⁻¹ has a CCPP of 10.9 ng PIC during a week of growth (**Figure 9B**). To directly compare responses of cellular calcification rates and the CaCO₃ production potential (CCPP) of a community to rising *f*CO₂, both measures were normalized to respective values at 280 μatm. For instance, an increase to 1,000 μatm drops cellular calcification rates to about 45% of the rate observed at 280 μatm (**Figure 9C**) while CCPP of a community would be reduced to 10%.

4. DISCUSSION

4.1. Equation Fit and Working Limits

Previously, analytical equations would have to run a separate fit for carbonate chemistry effects under each temperature and light condition (i.e., Sett et al., 2014; Zhang et al., 2015). By accounting for combined changes in light, temperature and carbonate chemistry fit Equation (8) was able to explain up to 88% of variability in measured rates. Rates were stimulated by increasing light intensities up to saturating light, beyond this point rates decreased slightly as light became inhibiting (**Figure 4**). The stimulating effects of light depended upon *f*CO₂, with light having weaker stimulating effects on rates at higher *f*CO₂ levels (**Figure 4**). Rates were also stimulated by temperature with rates increasing from limiting low temperatures up to an optimum, beyond this point rates decreased as temperatures became inhibiting (**Table 4**). The magnitude of stimulation by temperature depended upon CO₂, with the greatest stimulation by temperature observed in the optimal CO₂ range between 5 and 30 μmol kg⁻¹ (**Figure 5**). Increasing substrate availability at low CO₂ resulted in rapid increases in metabolic rates, while increasing H⁺ at high CO₂ resulted in the inhibition and decrease of metabolic rates (**Figure 5**).

In an attempt to estimate the significance of the observation that individual metabolic rates appear to have different CO₂ requirements for optimum rates, and sensitivities concerning half saturation and inhibition (e.g., compare **Table 5**), a single fit to a combined data-set of normalized (to individual maxima) rates for growth, calcification and photosynthesis was applied. The fact that this single fit explained at best less than half of the variation in the data in comparison to the individual ones suggests that metabolic rates should be treated separately as having specific sensitivities and requirements.

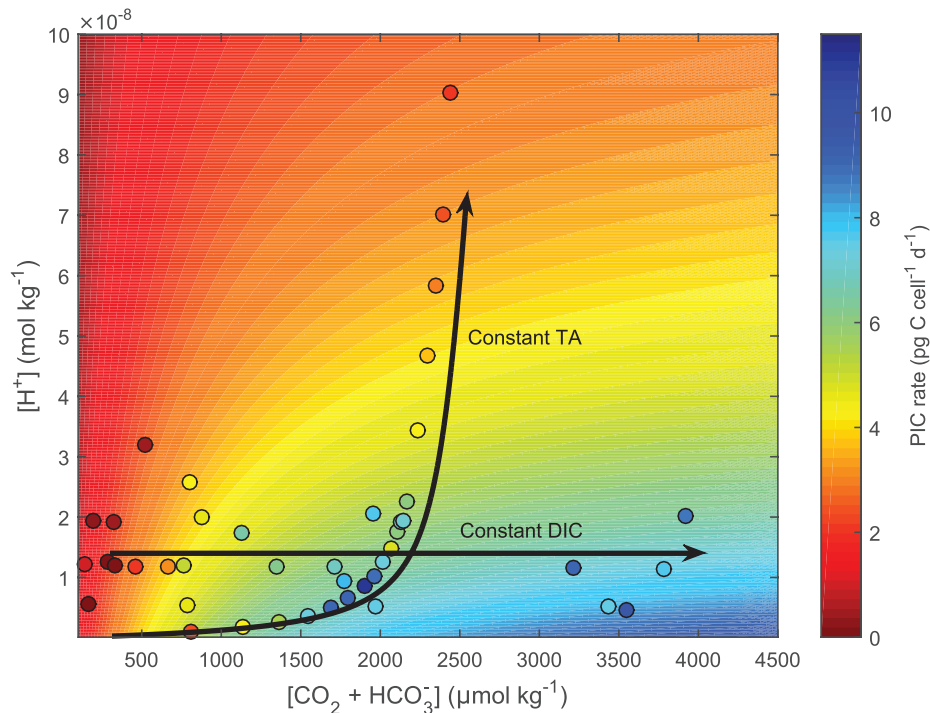


FIGURE 7 | Test of the ability of Equation (8) to fit responses to coupled and decoupled carbonate chemistry systems using *E. huxleyi*. Contour lines were produced using Equation (8) and fit coefficients derived from *E. huxleyi* data presented in Bach et al. (2015) (see section 2.9 for details). Colors indicate projected (contour lines) and measured (dots) calcification rates. Lines highlight carbonate chemistry conditions for coupled (constant TA) and decoupled (constant pH) systems.

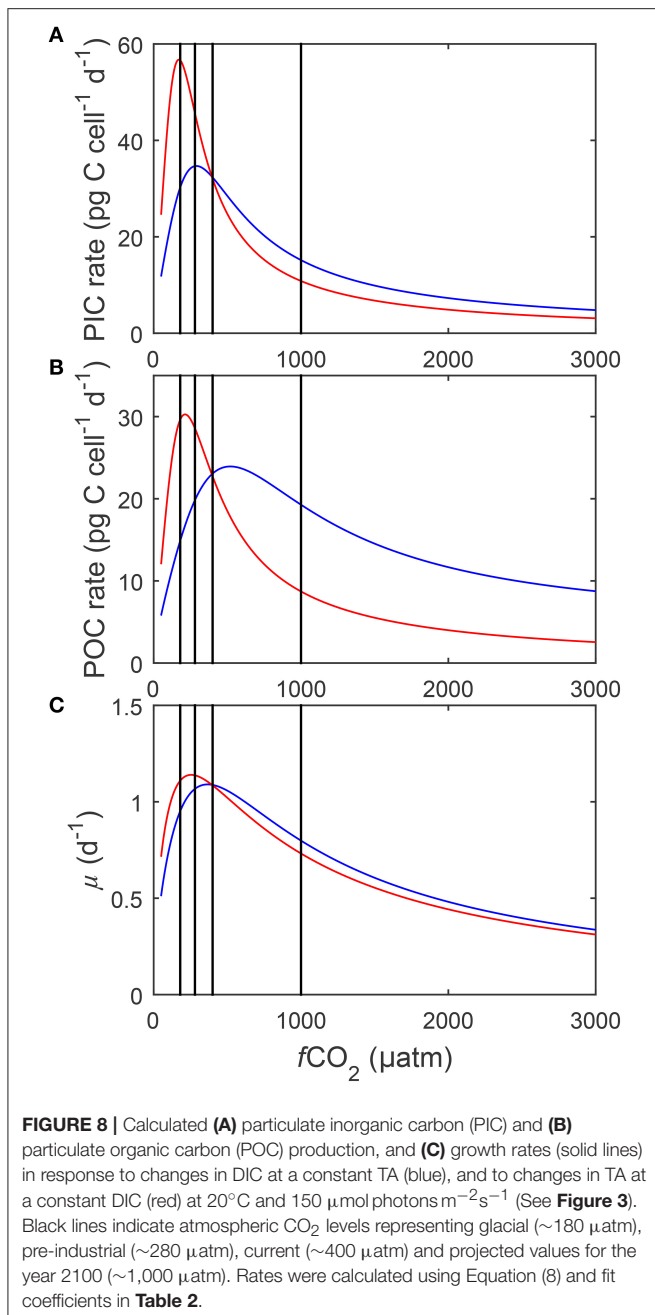
Combinations of extreme environmental values outside the existing experimental data ranges ($15 < T(^{\circ}\text{C}) < 25$, $20 < f\text{CO}_2(\mu\text{atm}) < 3,500$, $50 < I(\mu\text{mol photons m}^{-2} \text{s}^{-1}) < 800$), resulted in a decreased ability of the equation to project physiological responses. Temperatures below $11\text{--}12^{\circ}\text{C}$ resulted in a loss of light and CO_2 inhibition, while $f\text{CO}_2$ levels above $2,000\text{--}3,000 \mu\text{atm}$ resulted in a slight overestimation of rates at combined high light-temperature. Growth rates at low light intensities and $f\text{CO}_2$ levels below $100 \mu\text{atm}$ lacked light limitation. Acknowledging these limitations, the working range for the current fit is restricted to temperatures above 11°C and $f\text{CO}_2$ levels below $2,000 \mu\text{atm}$ for calcification, above 12°C and $f\text{CO}_2$ levels below $3,000 \mu\text{atm}$ for photosynthetic rates, and above 12°C and between 100 and $3,000 \mu\text{atm}$ for growth rates. These limitations are most likely the result of model projections well outside the original data range at combinations of high/low temperature, light and CO_2 . However, within the data range of environmental input parameters, Equation (8) allows calculation and projection of metabolic rates outside the limited experimental combinations of light, temperature and carbonate chemistry.

4.2. Interaction of Light, Temperature and Carbonate Chemistry in Modulating Physiological Rates

Light, temperature and carbonate chemistry have long been considered important factors in influencing metabolic rates

(Bopp et al., 2001; Sarmiento et al., 2004; Feng et al., 2008). Metabolic rates in *G. oceanica* double as temperature increases from 15°C to 25°C , increases fivefold as light increases from 50 to $800 \mu\text{mol photons m}^{-2} \text{s}^{-1}$, and vary fivefold over a CO_2 range of $25\text{--}3,500 \mu\text{atm}$ (Sett et al., 2014; Zhang et al., 2015). Similar effects of temperature, light and CO_2 have been observed for another coccolithophore, *Emiliania huxleyi*, where metabolic rates double as temperature increases from 10°C to 20°C (Sett et al., 2014), vary threefold over a CO_2 range of $20\text{--}6,000 \mu\text{atm}$ (Sett et al., 2014), and increases fivefold over a light range of $15\text{--}150 \mu\text{mol photons m}^{-2} \text{s}^{-1}$ (Rost et al., 2002). Based on this information, changes in light and temperature over an environmentally relevant range are able to influence metabolic rates at least as much as broad range carbonate chemistry. In fact when the effects of light and temperature were not included in our fit, (i.e., Equation 9) only 48% of the variability in measured metabolic rates was explained. This supports the notion that some of the discrepancies observed in the response of coccolithophores to ocean acidification are a result of differences in culturing conditions (including temperature, light) between different studies (Hoppe et al., 2011; Raven and Crawford, 2012; Rokitta and Rost, 2012; Sett et al., 2014).

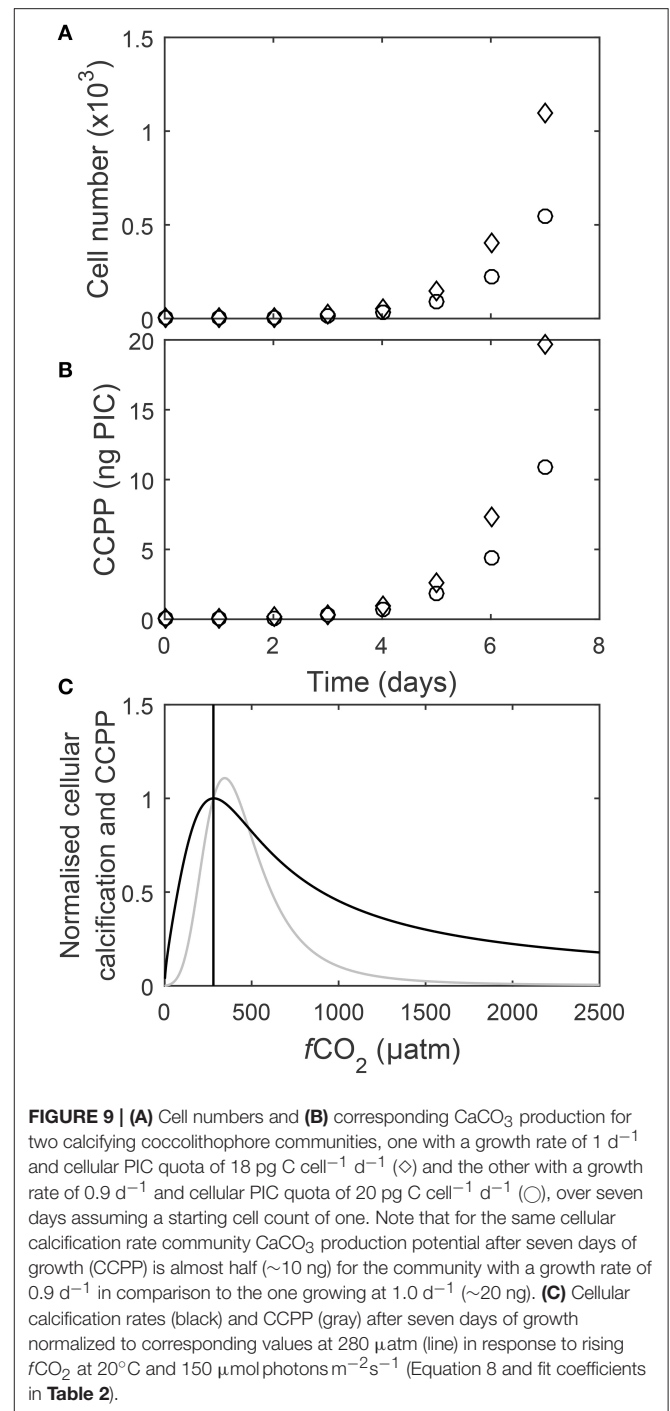
Strain may also be contributing to the above mentioned discrepancies. Significant differences have been observed between different strains of the same species when cultured under the same conditions (See Langer et al., 2009; Diner et al., 2015). As such, strain may also be an important factor to be



considered. More detailed information on the sensitivity and response of different strains to changing carbonate chemistry, temperature and light would be required before further efforts to account for these strain-specific differences could be made.

4.2.1. Light Responses

Calcification in *Gephyrocapsa oceanica* required higher light intensities, to reach maximum rates, than photosynthesis for the same $f\text{CO}_2$ level (**Figure 4**, **Table 3**). In contrast, *E. huxleyi* appears to saturate at much lower light intensities and shows either no difference in light saturation between processes (Rost



et al., 2002), or a higher light requirement for photosynthesis than calcification (van Bleijswijk et al., 1994) depending upon the strain examined. This could reflect a difference in light sensitivity of different metabolic processes between the two species.

Among the three rates, growth had the most rapid increase in rates from low to saturating light, the lowest light requirement to bring rates up to half of their maximum ($K_{\frac{1}{2}PAR}$ sat in **Table 3**), and the least change in rates from saturating to high

light intensities (**Figure 4C**). As cell division is critical for the survival of a coccolithophore population it appears reasonable to invest into growth over calcification and photosynthesis under sub-optimal light conditions.

Energy requirements for optimal rates declined with increasing $f\text{CO}_2$ for calcification and photosynthesis but increased with increasing $f\text{CO}_2$ for growth (**Table 3**). These results partly agree with the extrapolations made in Zhang et al. (2015), where light requirements for all optimum rates, decreased with increasing $f\text{CO}_2$. This indicates that as $f\text{CO}_2$ levels increase (at least up to 1,500 μatm), less energy is required for carbon production but more is required for maintaining cellular division. Energy requirements for both growth and calcification cover a similar range between 500 and 1,500 $f\text{CO}_2$. For photosynthesis however, light requirements for maximum rates are halved at 1,500 μatm in comparison to 500 μatm . It may be that increased $f\text{CO}_2$, through increased substrate availability, reduces the need for CO_2 concentrating mechanisms (CCMs) (Jin et al., 2013). As CCMs require energy to function, a reduction in their activity would result in a lower energy demand (Barcelos e Ramos et al., 2010), and therefore a lower light requirement for photosynthesis, and to a lesser degree calcification (Jin et al., 2013). The dependence of light responses on $f\text{CO}_2$ could have important implications for coccolithophores under future ocean conditions where both $f\text{CO}_2$ and light availability is expected to change. As energy requirements for cellular processes decrease, more energy may be diverted into resisting the negative effects of increasing $f\text{CO}_2/[\text{H}^+]$. For example more energy may be put into removal of excess H^+ from the cell (Barcelos e Ramos et al., 2010).

As $f\text{CO}_2$ levels rise and pH becomes more unfavorable, overall lower maximum rates are observed for the same light intensities (**Figure 4**). This effect, was stronger for calcification and photosynthetic rates than for growth rates (**Figure 4, Table 3**). Furthermore, rates vary much less with light at higher $f\text{CO}_2$ than at lower $f\text{CO}_2$ (**Figure 4**). This may indicate that at unfavorable CO_2/pH conditions coccolithophores sacrifice optimal carbon production in order to maintain steady growth rates which are essential for survival.

4.2.2. Temperature Responses

Temperature was observed to influence calcification, photosynthetic and growth rate responses of *G. oceanica*. Sensitivity of all rates was similar with optima at 23–25°C, half-saturation ($K_{\frac{1}{2}\text{Temp}}^{\text{sat}}$) at 15–17°C and half-inhibition ($K_{\frac{1}{2}\text{Temp}}^{\text{inhib}}$) at 29–31°C (**Table 4**). However, this finding should be considered with caution as rate measurements for only three temperatures were available.

Based on the fit, it would appear that temperature does not significantly influence responses to changing carbonate chemistry. At least until temperatures begin to approach the physiological limits for the species. CO_2 requirements for both optimal and half-saturation of rates tended to decrease with increasing temperatures (**Table 5**). However, these changes were generally small ($<12 \mu\text{mol kg}^{-1}$) most likely not significant in terms of cell physiology (**Table 5**). This indicates that between 15 and 25°C CO_2 requirements, at least from limiting to optimal

CO_2 , are practically insensitive to temperature. In contrast, CO_2 concentrations at which rates were half-inhibited by H^+ ($K_{\frac{1}{2}\text{CO}_2}^{\text{inhib}}$) were influenced by temperature, with higher CO_2/H^+ concentrations required to inhibit rates at 15°C than between 20 and 25°C (**Table 5, Figure 5**). The influence of temperature on metabolic rates also varied with temperature, with greater stimulation of rates observed at 20 and 25°C than at 15°C (**Table 5, Figure 5**). As 15°C is closer to the lower temperature limit for this strain, rates are likely being more strongly dictated by temperature than by changing CO_2 in this treatment. In particular, optimum rates appear much less sensitive to CO_2 changes, possibly because cultures can not take full advantage of ideal carbonate chemistry conditions when exposed to more unfavorable temperatures. This, combined with the results observed for light, where rates were lower and varied less with light at higher $f\text{CO}_2$ than at lower $f\text{CO}_2$, indicates that if one of the major factors for growth (i.e., CO_2 , temperature, light) becomes unfavorable, then rates will be depressed regardless of how optimal the other conditions might be. In other words, it becomes the dominant factor affecting rates. Furthermore, the limiting effects of extreme temperature and CO_2 conditions do not appear to be able to be compensated for by improvements in the non-limiting factors.

In terms of temperature- CO_2 response, our results (**Figure 5**) are similar to the fit observations produced by the original equation in Sett et al. (2014). Like Sett et al. (2014) we observed only small shifts in optimum CO_2 concentrations with increasing temperature ($<12 \mu\text{mol kg}^{-1}$) for all rates. So temperature appears to not significantly influence CO_2 optima for this species. A point of difference between the equations is that Sett's observed no influence of temperature on inhibition ($K_{\frac{1}{2}\text{CO}_2}^{\text{inhib}}$) whereas ours (Equation 8) observed an increase in H^+ inhibition with temperature (**Table 5**). However, our equation gives a non-linear rate change at high CO_2 , whereas the one in Sett had a relatively linear rate change. So it is likely that this discrepancy is a result of the different fitting capabilities of the two model equations.

4.2.3. Effects of Carbonate Chemistry on Cellular Processes

For a given temperature the CO_2 requirement for optimum rates is lowest for calcification and highest for photosynthesis (**Figure 5**). Additionally, calcification rates are more quickly inhibited toward higher pH than either growth or photosynthetic rates (**Table 5, Figure 5**). Differences in sensitivity to limitation ($K_{\frac{1}{2}\text{CO}_2}^{\text{sat}}$) between the three processes was small ($<1 \mu\text{mol kg}^{-1}$) and are therefore unlikely to be of physiological significance (**Table 5**).

Together these results indicate that calcification has a much higher sensitivity to $[\text{H}^+]$ ($K_{\frac{1}{2}\text{CO}_2}^{\text{inhib}}$) than either growth rates or photosynthesis. Similar results have been observed for *Emiliania huxleyi*, i.e., higher $[\text{H}^+]$ sensitivities than those for photosynthesis or growth (Bach et al., 2011; Sett et al., 2014). Experiments with *Coccolithus pelagicus* also found a higher sensitivity of calcification to $[\text{H}^+]$ (Bach et al., 2015). This suggests that in coccolithophores, calcification is the

most sensitive process to elevated $[H^+]$ /lowered pH. The sensitivity of calcification to elevated $[H^+]$ could be explained by a combination of internal acidification potentially reducing $[CO_3^{2-}]$ in the coccolith production vesicle (CPV) (Bach et al., 2013), and H^+ inhibition of HCO_3^- transport into the cell (Kottmeier et al., 2016a). In contrast, the sensitivity of other process to $[H^+]$ may be less direct. For example high $[H^+]$ can decrease HCO_3^- uptake and increase CO_2 uptake (Kottmeier et al., 2016b). Hence calcification, which is thought more dependent on $[HCO_3^-]$, could be expected to decrease while photosynthesis, which can utilize $[HCO_3^-]$ and $[CO_2]$ more equally, would likely be less impacted. As such it may be that the difference in sensitivity between calcification and photosynthesis is the result of slightly different substrate dependencies.

The results also indicate that calcification has a slightly lower requirement for substrate (CO_2 and HCO_3^-), in terms of both optimum and $K_{\frac{1}{2}CO_2}$ sat, than either growth rates or photosynthesis. Similar results have been observed for *Emiliania huxleyi*, with lower optimum $[CO_2]$ than those for photosynthesis or growth (Bach et al., 2011; Sett et al., 2014). An alternate explanation is that the higher sensitivity of calcification to $[H^+]$ is shifting its substrate optima down to lower CO_2/H^+ concentrations. This is supported by experiments on *E. huxleyi*, in which the CO_2 optimum for calcification was higher under decoupled carbonate chemistry conditions (increasing CO_2 and constant H^+) than under coupled carbonate chemistry conditions (increasing CO_2 and H^+) (Bach et al., 2011, 2013). This again supports the notion that, calcification is the most sensitive process to elevated $[H^+]$.

4.3. Coupled and Decoupled Carbonate Systems

To test whether our conceptual model (Equation 8) could correctly fit responses to decoupled carbonate chemistry if data was available, it was applied to a combination of decoupled and coupled data of *E. huxleyi* used in Bach et al. (2015) at constant light and temperature. For coupled carbonate systems (Constant TA) rates showed an optimum curve response (See constant TA line in Figure 7), while the decoupled carbonate chemistry system showed a Michaelis-Menten response curve (See constant pH line in Figure 7). The mechanisms behind these responses are as follows. In both the coupled and decoupled carbonate chemistry system, low CO_2 (substrate) concentrations limit rates (Bach et al., 2011). As a result increased availability of CO_2 (substrate) stimulates rates in both scenarios (Figure 7). This stimulating effect decreases as CO_2 (substrate) concentrations approach saturating concentrations. It is at this point the two systems begin to diverge. In the coupled carbonate chemistry system as $[CO_2]$ further increase so do the concentrations of inhibiting H^+ (Bach et al., 2011, 2013). There comes a point where the inhibiting effect of rising $[H^+]$ overcomes the stimulating effect of CO_2 resulting in a decrease in rates (See constant TA line in Figure 7). Meanwhile in the decoupled carbonate chemistry system, H^+ does not change with rising CO_2 so rates remain constant with rising CO_2 once CO_2 saturation

is achieved (See constant pH line in Figure 7) (Bach et al., 2011, 2013). Measured calcification rate responses for *E. huxleyi* under coupled and decoupled carbonate chemistry conditions (See datapoints Figure 7), agree with the projections indicating that the fit equation is able to provide good estimates for both coupled and decoupled carbonate systems.

4.4. DIC vs. TA Manipulation

Higher maximum rates and lower fCO_2 optima were calculated for all processes in the constant DIC compared to the constant TA manipulation (Figure 8). This difference in absolute rates seems to be connected to the optimal CO_2 level of each process, i.e., the further away it is from $400 \mu atm$ (the point at which both manipulation methods were set to result in exactly the same carbonate chemistry), the more pronounced the difference in calculated rates. Below $400 \mu atm$ the only substantial difference in carbonate chemistry speciation between the manipulation methods is in the concentration of HCO_3^- (Figure 3). The difference in HCO_3^- concentration between the methods was greatest at the lowest fCO_2 concentrations and decreased as fCO_2 levels approached $400 \mu atm$. The optimum of calcification, being at the lowest fCO_2 (Figure 8), coincided with the largest difference in $[HCO_3^-]$ between the two methods resulting in the most substantial difference in calculated rates (Figure 3). The optimum for photosynthesis, being slightly higher, occurred at a lower HCO_3^- difference which resulted in a lower difference in calculated rates. Finally the optimum for growth occurred at the highest fCO_2 levels where there was comparatively little difference in $[HCO_3^-]$ between the methods resulting in little differences in calculated rates. As such it is likely that the differences in overall rate and fCO_2 optimum are being driven by differences in $[HCO_3^-]$.

Physiological rates at constant DIC were consistently lower than at constant TA at fCO_2 levels above $500 \mu atm$ (Figure 8). Above $500 \mu atm$ the only substantial difference in carbonate chemistry between the manipulation methods was again in the concentration of HCO_3^- which was consistently higher in the constant TA manipulation (Figure 3). Higher $[HCO_3^-]$ has been shown to be able to compensate for the inhibiting effects of unfavorable H^+ (Bach et al., 2013). As such the TA manipulation, with higher $[HCO_3^-]$ at the same fCO_2 when above $400 \mu atm$, would be expected to have higher overall rates.

A significant impact of differing HCO_3^- concentrations on measured metabolic rates in constant DIC versus constant TA manipulations have previously been estimated to occur below 80 and higher than $700 \mu atm$ (Schulz et al., 2009). Here, however, it was found that the further the optimum CO_2 of a process is away from $400 \mu atm$ (the point at which both manipulation methods were set to result in exactly the same carbonate chemistry), the larger the differences can become. This will be difficult to detect experimentally, however, when not employing a larger fCO_2 treatment range with relatively high resolution, although certain evidence appears to exist for *Emiliania huxleyi* (Hoppe et al., 2011). It is reiterated though that overall response patterns to fCO_2 are not affected by the carbonate chemistry manipulation method chosen.

4.5. Community Calcification Potential

Potential impacts of ocean acidification on coccolithophorid calcification is typically assessed by comparing changes in cellular calcification rates and PIC:POC ratios. Calcification rates however, depend on both cellular growth rates and CaCO_3 quotas which usually change independently. In two communities with identical cellular calcification rates, the one with the higher growth rate will produce twice the cellular standing stock and 1.8 times the CaCO_3 as the community with the lower growth rate (**Figures 9A,B**). This exercise illustrates that when assessing potential impacts on communities, growth rates are key. This is supported by the recent finding that the ability of coccolithophores to form blooms can be severely impacted toward higher CO_2 levels (Riebesell et al., 2017).

To assess the impact of increasing $f\text{CO}_2$ on calcification of coccolithophorids on the community level it appears crucial to explicitly factor in cellular growth rates and use a measure like the CaCO_3 community production potential (CCPP), for instance for a growth period of seven days. A direct comparison between CCPP and cellular calcification rates in response to increasing $f\text{CO}_2$ is then obtained by normalizing them to respective values for, for instance, pre-industrial levels of $280 \mu\text{atm}$. Normalized CCPP had a slightly higher $f\text{CO}_2$ optimum (at about $345 \mu\text{atm}$) than normalized cellular calcification rates (at about $282 \mu\text{atm}$) (**Figure 9C**). Furthermore, normalized CCPP exceeded pre-industrial carbon production over a range of $\sim 280\text{--}500 \mu\text{atm}$ (**Figure 9C**). However, normalized CCPP decreases much more rapidly above and below this optimum $f\text{CO}_2$ than normalized cellular calcification rates (**Figure 9C**). For example at $750 \mu\text{atm}$ normalized CCPP is only $\sim 28\%$ compared to pre-industrial levels, while normalized cellular calcification is $\sim 60\%$. Furthermore, while cellular calcification rates at $1,000 \mu\text{atm}$ are still about half of those at pre-industrial CO_2 levels, CaCO_3 community production potential is only about a tenth in comparison to pre-industrial times. Finally, the differences in response between cellular calcification and CCPP become even more pronounced if longer growth periods (i.e., longer than the 7 days chosen here) are considered. This indicates that CaCO_3 production by coccolithophores on the global scale could be much more impacted by the end of this century than suggested when comparing changes in cellular calcification rates. The reason for these differences is that CCPP factors in the impacts of growth rates on cell densities in an exponentially growing community whereas cellular calcification rates do not. In fact, CCPP and cellular calcification rates would be identical if changes were due to changes in CaCO_3 quotas only with no effect on growth rates. As this is clearly not the case, cellular calcification rates can be a poor measure of CaCO_3 production capacity at the community level. For future projections it will also be important to factor in other environmental variables as well as species competition and interaction which appears to be a major factor controlling phytoplankton standing stocks in large parts of the ocean (Behrenfeld, 2014).

5. CONCLUSIONS

Future global change is expected to impact ocean carbonate chemistry, temperature and light conditions at the same time (IPCC, 2013a). Changes in temperature, carbonate chemistry and light have all been observed to significantly influence growth, calcification and photosynthetic rates of coccolithophores (Bach et al., 2011; Sett et al., 2014; Zhang et al., 2015). The conceptual model and its resulting fit equation developed in this study is able to account for the effects of temperature and light inhibition and limitation, as well as the balance of stimulating (CO_2 and HCO_3^-) and inhibiting (H^+) effects of changing carbonate chemistry. Therefore, it combines the functionality of previous analytical equations (i.e., Bach et al., 2015) in fitting carbonate chemistry responses with the ability to account for the effects of simultaneous changes in temperature and light conditions. As such this equation represents a step forward in our ability to describe coccolithophore responses to changes in multiple environmental variables. Given the fundamentals of stimulation and inhibition by environmental factors, these equations should also be applicable to other autotrophic organisms for growth and photosynthesis.

Calculations suggest that a single unfavorable growth condition (CO_2 , temperature, light, nutrients) will control absolute rates and result in decreased sensitivity to changes in other environmental variables. Calculations also suggest that growth, calcification and photosynthesis may have very different sensitivities to $[\text{H}^+]$, substrate and light availability. Of the three rates calcification was found to be most sensitive to the effects of increasing H^+ , to have the highest light requirement and the lowest substrate requirement. Finally calculations suggest that cellular calcification rates alone underestimate the sensitivity of coccolithophore production on the community level to changes in $f\text{CO}_2$. Therefore we introduce a new metric, CaCO_3 production potential (CCPP), which factors in the impact of growth rates on cell densities in an exponentially growing community.

AUTHOR CONTRIBUTIONS

KS, NG, and BE: Conceived and designed the experiments; NG, Performed the experiments; NG and KS: Analyzed the data; NG, KS, and BE: Wrote the paper.

ACKNOWLEDGMENTS

This study was funded by the Australian Research Council (ARC) FT120100384 awarded to KS and DP150102092 awarded to BE and KS.

SUPPLEMENTARY MATERIAL

The Supplementary Material for this article can be found online at: <https://www.frontiersin.org/articles/10.3389/fmars.2017.00433/full#supplementary-material>

REFERENCES

- Armstrong, R. A., Lee, C., Hedges, J. I., Honjo, S., and Wakeham, S. G. (2002). A new, mechanistic model for organic carbon fluxes in the ocean based on the quantitative association of POC with ballast minerals. *Deep Sea Res. II Top. Stud. Oceanogr.* 49, 219–236. doi: 10.1016/S0967-0645(01)00101-1
- Bach, L. T., MacKinder, L. C. M., Schulz, K. G., Wheeler, G., Schroeder, D. C., Brownlee, C., et al. (2013). Dissecting the impact of CO₂ and pH on the mechanisms of photosynthesis and calcification in the coccolithophore *Emiliania huxleyi*. *New Phytol.* 199, 121–134. doi: 10.1111/nph.12225
- Bach, L. T., Riebesell, U., Gutowska, M. A., Federwisch, L., and Schulz, K. G. (2015). A unifying concept of coccolithophore sensitivity to changing carbonate chemistry embedded in an ecological framework. *Progr. Oceanogr.* 135, 125–138. doi: 10.1016/j.pocean.2015.04.012
- Bach, L. T., Riebesell, U., and Schulz, K. G. (2011). Distinguishing between the effects of ocean acidification and ocean carbonation in the coccolithophore *Emiliania huxleyi*. *Limnol. Oceanogr.* 56, 2040–2050. doi: 10.4319/lo.2011.56.6.2040
- Barcelos e Ramos, J., Müller, M. N., and Riebesell, U. (2010). Short-term response of the coccolithophore *Emiliania huxleyi* to an abrupt change in seawater carbon dioxide concentrations. *Biogeosciences* 7, 177–186. doi: 10.5194/bg-7-177-2010
- Beaufort, L., and Heussner, S. (1999). Coccolithophorids on the continental slope of the Bay of Biscay—production, transport and contribution to mass fluxes. *Deep Sea Res. II* 46, 2147–2174. doi: 10.1016/S0967-0645(99)00058-2
- Behrenfeld, M. J. (2014). Climate-mediated dance of the plankton. *Nat. Clim. Change* 4, 880–887. doi: 10.1038/nclimate2349
- Bopp, L., Monfray, P., Aumont, O., Dufresne, J.-L., Le Treut, H., Madec, G., et al. (2001). Potential impact of climate change on marine export production. *Glob. Biogeochem. Cycles* 15, 81–99. doi: 10.1029/1999GB001256
- Broecker, W., and Clark, E. (2009). Ratio of coccolith CaCO₃ to foraminifera CaCO₃ in late Holocene deep sea sediments. *Paleoceanography* 24:PA3205. doi: 10.1029/2009PA001731
- Buitenhuis, E. T., Pangerc, T., Franklin, D. J., Le Quère, C., and Malin, G. (2008). Growth rates of six coccolithophorid strains as a function of temperature. *Limnol. Oceanogr.* 53, 1181–1185. doi: 10.4319/lo.2008.53.3.1181
- Burkhardt, S., Amoroso, G., Riebesell, U., and Sltmeyer, D. (2001). CO₂ and HCO₃⁻ uptake in marine diatoms acclimated to different CO₂ concentrations. *Limnol. Oceanogr.* 46, 1378–1391. doi: 10.4319/lo.2001.46.6.1378
- Burkhardt, S., Riebesell, U., and Zondervan, I. (1999). Effects of growth rate, CO₂ concentration, and cell size on the stable carbon isotope fractionation in marine phytoplankton. *Geochim. Cosmochimica Acta* 63, 3729–3741. doi: 10.1016/S0016-7037(99)00217-3
- Caldeira, K., and Wickett, M. E. (2005). Ocean model predictions of chemistry changes from carbon dioxide emissions to the atmosphere and ocean. *J. Geophys. Res.* 110:C09S04. doi: 10.1029/2004JC002671
- Charalampopoulou, A. (2011). *Coccolithophores in High Latitude and Polar Regions: Relationships between Community Composition, Calcification and Environmental Factors*. Southampton: Doctor of Philosophy, School of Ocean and Earth Science.
- Coleman, J. R., and Colman, B. (1981). Inorganic carbon accumulation and photosynthesis in a blue-green alga as a function of external pH. *Plant Physiol.* 67, 917–921. doi: 10.1104/pp.67.5.917
- de Vargas, C., Aubry, M. P., Probert, I., Young, J., Falkowski, P., and Knoll, A. H. (2007). “Origin and evolution of coccolithophores: from coastal hunters to oceanic farmers,” in *Evolution of Aquatic Photoautotrophs*, book section 12, eds P. Falkowski and A. H. Knoll (New York, NY: Elsevier Academic Press), 251–281.
- Dickson, A. G., Wesolowski, D. J., Palmer, D. A., and Mesmer, R. E. (1990). Dissociation constant of bisulfate ion in aqueous sodium chloride solutions to 250°C. *J. Phys. Chem.* 94, 7978–7985. doi: 10.1021/j100383a042
- Diner, R. E., Benner, L., Passow, U., Komada, T., Carpenter, E. J., and Stillman, J. H. (2015). Negative effects of ocean acidification on calcification vary within the coccolithophore genus *Calcidiscus*. *Mar. Biol.* 162, 1287–1305. doi: 10.1007/s00227-015-2669-x
- Doney, S. C., Fabry, V. J., Feely, R. A., and Kleypas, J. A. (2009). Ocean acidification: the other CO₂ problem. *Annu. Rev. Mar. Sci.* 1, 169–192. doi: 10.1146/annurev.marine.010908.163834
- Eppley, R. W. (1972). Temperature and phytoplankton growth in the sea. *Fish. Bull.* 70, 1063–1085.
- Farazdaghi, H. (2011). The single-process biochemical reaction of Rubisco: a unified theory and model with the effects of irradiance, CO₂ and rate-limiting step on the kinetics of C₃ and C₄ photosynthesis from gas exchange. *Biosystems* 103, 265–284. doi: 10.1016/j.biosystems.2010.11.004
- Feng, Y., Warner, M. E., Zhang, Y., Sun, J., Fu, F.-X., Rose, J. M., et al. (2008). Interactive effects of increased pCO₂, temperature and irradiance on the marine coccolithophore *Emiliania huxleyi* (Prymnesiophyceae). *Eur. J. Phycol.* 43, 87–98. doi: 10.1080/09670260701664674
- Helm, D., Cook, S., Cubillos, J., McMinn, A., and Hallegraef, G. M. (2007). *Growth, Photosynthesis and Temperature Tolerance of Eight Southern Ocean Strains of the Coccolithophorid Emiliania huxleyi*. Thesis, Institute of Antarctic and Southern Ocean Studies.
- Herfort, L., Loste, E., Meldrum, F., and Thake, B. (2004). Structural and physiological effects of calcium and magnesium in *Emiliania huxleyi* (Lohmann) Hay and Mohler. *J. Struct. Biol.* 148, 307–314. doi: 10.1016/j.jsb.2004.07.005
- Holligan, P. M., Fernández, E., Aiken, J., Balch, W. M., Boyd, P., Burkill, P. H., et al. (1993a). A biogeochemical study of the coccolithophore, *Emiliania huxleyi*, in the North Atlantic. *Glob. Biogeochem. Cycles* 7, 879–900.
- Holligan, P. M., Groom, S. B., and Harbour, D. S. (1993b). What controls the distribution of the coccolithophore, *Emiliania huxleyi*, in the North Sea? *Fish. Oceanogr.* 2, 175–183.
- Holtz, L.-M., Wolf-Gladrow, D., and Thoms, S. (2015a). Numerical cell model investigating cellular carbon fluxes in *Emiliania huxleyi*. *J. Theor. Biol.* 364, 305–315. doi: 10.1016/j.jtbi.2014.08.040
- Holtz, L.-M., Wolf-Gladrow, D., and Thoms, S. (2015b). Simulating the effects of light intensity and carbonate system composition on particulate organic and inorganic carbon production in *Emiliania huxleyi*. *J. Theor. Biol.* 372, 192–204. doi: 10.1016/j.jtbi.2015.02.024
- Hoppe, C. J. M., Langer, G., and Rost, B. (2011). *Emiliania huxleyi* shows identical responses to elevated pCO₂ in TA and DIC manipulations. *J. Exp. Mar. Biol. Ecol.* 406, 54–62. doi: 10.1016/j.jembe.2011.06.008
- IPCC (2013a). *Climate Change 2013: The Physical Science Basis. Contribution of Working Group I to the Fifth Assessment Report of the Intergovernmental Panel on Climate Change*. Cambridge, New York, NY: Cambridge University Press.
- IPCC (2013b). “Summary for policy makers,” in *Climate Change 2013: The Physical Science Basis. Contribution of Working Group I to the Fifth Assessment Report of the Intergovernmental Panel on Climate Change*, eds T. F. Stocker, D. Qin, G.-K. Plattner, M. Tignor, S. K. Allen, J. Boschung, A. Nauels, Y. Xia, V. Bex, and P. M. Midgley (Cambridge; New York, NY: Cambridge University Press), 1–27.
- Jin, P., Gao, K., and Beardall, J. (2013). Evolutionary responses of a coccolithophorid *Gephyrocapsa oceanica* to ocean acidification. *Evolution* 67, 1869–1878. doi: 10.1111/evo.12112
- Keller, K., and Morel, F. M. (1999). A model of carbon isotopic fractionation and active carbon uptake in phytoplankton. *Mar. Ecol. Prog. Ser.* 182, 295–298. doi: 10.3354/meps182295
- Kottmeier, D. M., Rokitta, S. D., and Rost, B. (2016a). Acidification, not carbonation, is the major regulator of carbon fluxes in the coccolithophore *Emiliania huxleyi*. *New Phytol.* 211, 126–137. doi: 10.1111/nph.13885
- Kottmeier, D. M., Rokitta, S. D., and Rost, B. (2016b). H⁺-driven increase in CO₂ uptake and decrease in HCO₃⁻ uptake explain coccolithophores’ acclimation responses to ocean acidification. *Limnol. Oceanogr.* 61, 2045–2057. doi: 10.1002/lno.10352
- Kottmeier, D. M., Rokitta, S. D., Tortell, P. D., and Rost, B. (2014). Strong shift from HCO₃⁻ to CO₂ uptake in *Emiliania huxleyi* with acidification: new approach unravels acclimation versus short-term pH effects. *Photosynthesis Res.* 121, 265–275. doi: 10.1007/s11120-014-9984-9
- Langer, G., Nehrke, G., Probert, I., Ly, J., and Ziveri, P. (2009). Strain-specific responses of *Emiliania huxleyi* to changing seawater carbonate chemistry. *Biogeosci. Discuss.* 6, 4361–4383. doi: 10.5194/bgd-6-4361-2009
- Larsen, S. H. (2012). *Dimethylsulphoniopropionate (DMSP) Production of Gephyrocapsa oceanica in Response to Environmental Forcing*. Melbourne, VIC: Doctor of philosophy, School of Biological Sciences.
- Laws, E. A., Popp, B. N., Bidigare, R. R., Kennicutt, M. C., and Macko, S. A. (1995). Dependence of phytoplankton carbon isotopic composition on growth rate

- and [CO₂] aq: theoretical considerations and experimental results. *Geochim. Cosmochimica Acta* 59, 1131–1138. doi: 10.1016/0016-7037(95)00030-4
- Lewis, E., Wallace, D., and Allison, L. J. (1998). *Program Developed for CO₂ System Calculations*. Oak Ridge, TN: Carbon Dioxide Information Analysis Center, Managed by Lockheed Martin Energy Research Corporation for the US Department of Energy Tennessee.
- Lueker, T. J., Dickson, A. G., and Keeling, C. D. (2000). Ocean pCO₂ calculated from dissolved inorganic carbon, alkalinity, and equations for K₁ and K₂: validation based on laboratory measurements of CO₂ in gas and seawater at equilibrium. *Mar. Chem.* 70, 105–119. doi: 10.1016/S0304-4203(00)00022-0
- McIntyre, A., and Bé, A. W. H. (1967). Modern Coccolithophoridae of Atlantic Ocean -I. Placoliths and cyrtoliths. *Deep Sea Res. Oceanogr. Abstracts* 14, 561–597. doi: 10.1016/0011-7471(67)90065-4
- Megard, R. O., Tonkyn, D. W., and Senft, W. H. (1984). Kinetics of oxygenic photosynthesis in planktonic algae. *J. Plank. Res.* 6, 325–337. doi: 10.1093/plankt/6.2.325
- Nimer, N. A., and Merrett, M. J. (1993). Calcification rate in *Emiliania huxleyi* Lohmann in response to light, nitrate and availability of inorganic carbon. *New Phytol.* 123, 673–677. doi: 10.1111/j.1469-8137.1993.tb03776.x
- Norberg, J. (2004). Biodiversity and ecosystem functioning: a complex adaptive systems approach. *Limnol. Oceanogr.* 49, 1269–1277. doi: 10.4319/lo.2004.49.4_part_2.1269
- Orr, J. C., Fabry, V. J., Aumont, O., Bopp, L., Doney, S. C., Feely, R. A., et al. (2005). Anthropogenic ocean acidification over the twenty-first century and its impact on calcifying organisms. *Nature* 437, 681–686. doi: 10.1038/nature04095
- Paasche, E. (2001). A review of the coccolithophorid *Emiliania huxleyi* (Prymnesiophyceae), with particular reference to growth, coccolith formation, and calcification-photosynthesis interactions. *Phycologia* 40, 503–529. doi: 10.2216/10031-8884-40-6-503.1
- Pörtner, H. O., and Farrell, A. P. (2008). Physiology and climate change. *Science* 322, 690–692. doi: 10.1126/science.1163156
- Poulton, A. J., Adey, T. R., Balch, W. M., and Holligan, P. M. (2007). Relating coccolithophore calcification rates to phytoplankton community dynamics: regional differences and implications for carbon export. *Deep Sea Res. II Top. Stud. Oceanogr.* 54, 538–557. doi: 10.1016/j.dsr2.2006.12.003
- Poulton, A. J., Charalampopoulou, A., Young, J. R., Tarran, G. A., Lucas, M. I., and Quartly, G. D. (2010). Coccolithophore dynamics in non-bloom conditions during late summer in the central Iceland Basin (July–August 2007). *Limnol. Oceanogr.* 55, 1601–1613. doi: 10.4319/lo.2010.55.4.1601
- Powles, S. B. (1984). Photoinhibition of photosynthesis induced by visible light. *Annu. Rev. Plant Physiol.* 35, 15–44. doi: 10.1146/annurev.pp.35.060184.000311
- Raven, J. A., and Crawford, K. (2012). Environmental controls on coccolithophore calcification. *Mar. Ecol. Prog. Ser.* 470, 137–166. doi: 10.3354/meps09993
- Rhodes, L. L., Peake, B. M., MacKenzie, A. L., and Marwick, S. (1995). Coccolithophores *Gephyrocapsa oceanica* and *Emiliania huxleyi* (Prymnesiophyceae = Haptophyceae) in New Zealand's coastal waters: characteristics of blooms and growth in laboratory culture. *New Zeal. J. Mar. Freshw. Res.* 29, 345–357. doi: 10.1080/00288330.1995.9516669
- Rickaby, R. E. M., Henderiks, J., and Young, J. N. (2010). Perturbing phytoplankton: response and isotopic fractionation with changing carbonate chemistry in two coccolithophore species. *Clim. Past* 6, 771–785. doi: 10.5194/cp-6-771-2010
- Ridgwell, A. (2005). A Mid Mesozoic Revolution in the regulation of ocean chemistry. *Mar. Geol.* 217, 339–357. doi: 10.1016/j.margeo.2004.10.036
- Riebesell, U., Bach, L. T., Bellerby, R. G., Monsalve, J. R. B., Boxhammer, T., Czerny, J., et al. (2017). Competitive fitness of a predominant pelagic calcifier impaired by ocean acidification. *Nat. Geosci.* 10, 19–23. doi: 10.1038/ngeo2854
- Riebesell, U., Körtzinger, A., and Oschlies, A. (2009). Sensitivities of marine carbon fluxes to ocean change. *Proc. Natl. Acad. Sci. U.S.A.* 106, 20602–20609. doi: 10.1073/pnas.0813291106
- Rokitta, S. D., and Rost, B. (2012). Effects of CO₂ and their modulation by light in the life-cycle stages of the coccolithophore *Emiliania huxleyi*. *Limnol. Oceanogr.* 57, 607–618. doi: 10.4319/lo.2012.57.2.0607
- Rost, B., and Riebesell, U. (2004). “Coccolithophores and the biological pump: responses to environmental changes,” in *Coccolithophores: From Molecular Processes to Global Impacts*, book section 5, eds H. R. Thierstein and J. R. Young (Berlin; Heidelberg: Springer), 99–125.
- Rost, B., Riebesell, U., Burkhardt, S., and Sültemeyer, D. (2003). Carbon acquisition of bloom-forming marine phytoplankton. *Limnol. Oceanogr.* 48, 55–67. doi: 10.4319/lo.2003.48.1.0055
- Rost, B., Zondervan, I., and Riebesell, U. (2002). Light-dependent carbon isotope fractionation in the coccolithophorid *Emiliania huxleyi*. *Limnol. Oceanogr.* 47, 120–128. doi: 10.4319/lo.2002.47.1.0120
- Sarmiento, J. L., Slater, R., Barber, R., Bopp, L., Doney, S. C., Hirst, A., et al. (2004). Response of ocean ecosystems to climate warming. *Glob. Biogeochem. Cycles* 18:GB3003. doi: 10.1029/2003GB002134
- Schulz, K. G., Barcelos e Ramos, J., Zeebe, R. E., and Riebesell, U. (2009). CO₂ perturbation experiments: similarities and differences between dissolved inorganic carbon and total alkalinity manipulations. *Biogeochem. Discuss.* 6, 2145–2153. doi: 10.5194/bg-6-2145-2009
- Schulz, K. G., Rost, B., Burkhardt, S., Riebesell, U., Thoms, S., and Wolf-Gladrow, D. (2007). The effect of iron availability on the regulation of inorganic carbon acquisition in the coccolithophore *Emiliania huxleyi* and the significance of cellular compartmentation for stable carbon isotope fractionation. *Geochim. Cosmochimica Acta* 71, 5301–5312. doi: 10.1016/j.gca.2007.09.012
- Sett, S., Bach, L. T., Schulz, K. G., Koch-Klavsen, S., Lebrato, M., and Riebesell, U. (2014). Temperature modulates coccolithophorid sensitivity of growth, photosynthesis and calcification to increasing seawater pCO₂. *PLoS ONE* 9:e88308. doi: 10.1371/journal.pone.0088308
- Sharkey, T. D., and Berry, J. A. (1985). “Carbon isotope fractionation of algae as influenced by an inducible CO₂ concentrating mechanism,” in *Inorganic Carbon Uptake by Aquatic Photosynthetic Organisms: Proceedings of an International Workshop on Bicarbonate Use in Photosynthesis, August 18–22, 1984, Commemorating the Seventy-fifth Anniversary of the University of California, Davis, 1909–1984*, eds W. J. Lucas and J. A. Berry (Davis, CA: American Society of Plant Physiologists), 389–401.
- Suffrian, K., Schulz, K. G., Gutowska, M. A., Riebesell, U., and Bleich, M. (2011). Cellular pH measurements in *Emiliania huxleyi* reveal pronounced membrane proton permeability. *New Phytol.* 190, 595–608. doi: 10.1111/j.1469-8137.2010.03633.x
- Taylor, A. R., Chrachri, A., Wheeler, G., Goddard, H., and Brownlee, C. (2011). A voltage-gated H⁺ channel underlying pH homeostasis in calcifying coccolithophores. *PLoS Biol.* 9:e1001085. doi: 10.1371/journal.pbio.1001085
- Trimborn, S., Langer, G., and Rost, B. (2007). Effect of varying calcium concentrations and light intensities on calcification and photosynthesis in *Emiliania huxleyi*. *Limnol. Oceanogr.* 52, 2285–2293. doi: 10.4319/lo.2007.52.5.2285
- Uppström, L. R. (1974). The boron/chlorinity ratio of deep-sea water from the Pacific Ocean. *Deep Sea Res. Oceanogr. Abstracts* 21, 161–162. doi: 10.1016/0011-7471(74)90074-6
- van Bleijswijk, J. D. L., Kempers, R. S., and Velhuis, M. J. (1994). Cell and growth characteristics of types A and B of *Emiliania huxleyi* (Prymnesiophyceae) as determined by flow cytometry and chemical analysis. *J. Phycol.* 30, 230–241. doi: 10.1111/j.0022-3646.1994.00230.x
- von Dassow, P., van den Engh, G., Iglesias-Rodriguez, D., and Gittins, J. R. (2012). Calcification state of coccolithophores can be assessed by light scatter depolarization measurements with flow cytometry. *J. Plank. Res.* 34, 1011–1027. doi: 10.1093/plankt/fbs061
- Westbroek, P., Brown, C. W., van Bleijswijk, J., Brownlee, C., Brummer, G. J., Conte, M., et al. (1993). A model system approach to biological climate forcing. The example of *Emiliania huxleyi*. *Glob. Planet. Change* 8, 27–46. doi: 10.1016/0921-8181(93)90061-R
- Zhang, Y., Bach, L. T., Schulz, K. G., and Riebesell, U. (2015). The modulating influence of light intensity on the response of the coccolithophore *Gephyrocapsa oceanica* to ocean acidification. *Limnol. Oceanogr.* 60, 2145–2157. doi: 10.1002/lno.10161
- Zondervan, I., Zeebe, R. E., Rost, B., and Riebesell, U. (2001). Decreasing marine biogenic calcification: a negative feedback on rising atmospheric pCO₂. *Glob. Biogeochem. Cycles* 15, 507–516. doi: 10.1029/2000GB001321

Conflict of Interest Statement: The authors declare that the research was conducted in the absence of any commercial or financial relationships that could be construed as a potential conflict of interest.

Copyright © 2018 Gafar, Eyre and Schulz. This is an open-access article distributed under the terms of the Creative Commons Attribution License (CC BY). The use, distribution or reproduction in other forums is permitted, provided the original author(s) or licensor are credited and that the original publication in this journal is cited, in accordance with accepted academic practice. No use, distribution or reproduction is permitted which does not comply with these terms.